https://doi.org/10.5194/egusphere-2026-3689
Preprint. Discussion started: 28 July 2026

JULES-Palm: Explicit representation of oil palm plantations in a land surface model for estimating land-use change carbon emissions in Indonesia

Ida Bagus Mandhara Brasika[1,2], Pierre Friedlingstein[1,3], Stephen Sitch[4], Michael O'Sullivan[1], Maria Carolina Duran Rojas[1], Emma W. Littleton[1,4], Toby R. Marthews[5], Timothy Hill[4], Wei Li[6], Yidi Xu[7], Jiaxin Zhou[6], Xiangzhong Luo[8], Ruiying Zhao[8], Yuanchao Fan[9], Dedy Sukmara[10], Timer Manurung[10], Masayuki Kondo[11], Alexander Knohl[12], Tejaswini Jaajpera[12], Lisma Safitri[13,14]

[1] Department of Mathematics & Statistics, Faculty of Environment, Science & Economics, University of Exeter, Exeter, United Kingdom
[2] Department of Marine Science. Faculty of Marine Science & Fisheries, University of Udayana, Bali, Indonesia
[3] Laboratoire de Météorologie Dynamique, Institut Pierre-Simon Laplace, CNRS, École Normale Supérieure, Université PSL, Sorbonne Université, École Polytechnique, Paris, France
[4] Department of Geography, Faculty of Environment, Science & Economics, University of Exeter, Exeter, United Kingdom
[5] UK Centre for Ecology and Hydrology, Wallingford, United Kingdom
[6] Department of Earth System Science, Tsinghua University, Beijing, China
[7] Laboratoire des Sciences du Climat et de l'Environnement, LSCE/IPSL, CEA-CNRS-UVSQ, Université Paris Saclay, France
[8] Department of Geography, National University of Singapore, Singapore City, Singapore
[9] Institute of Environment and Ecology, Tsinghua Shenzhen International Graduate School, Tsinghua University, Shenzhen, China
[10] Auriga Nusantata, Bogor, Jawa Barat, Indonesia
[11] The IDEC Institute - Center for Peaceful and Sustainable Futures (CEPEAS), Network for Education and Research on Peace and Sustainability (NERPS), Seto Inland Sea Carbon Neutral Research Center (S-CNC), Graduate School of Humanities and Social Sciences International Economic Development Program (IEDP), Graduate School of Innovation and Practice for Smart Society (SmaSo), Hiroshima University, Higashi-Hiroshima, Japan
[12] Bioclimatology, University of Göttingen, Göttingen, Germany
[13] Stiper Agricultural University (Instiper Yogyakarta), Yogyakarta, Indonesia
[14] School of Earth and Environment, Univeristy of Leeds, Leeds, United Kingdom

Correspondence to: Ida Bagus Mandhara Brasika (i.brasika@exeter.ac.uk ; mandharabrasika@unud.ac.id)

Abstract. Expansion of oil palm plantations is a dominant driver of land-use change in equatorial Asia and has contributed substantially to deforestation in Indonesia. Most dynamic global vegetation models (DGVMs), however, still represent oil palm plantations as generic cropland, thereby contributing to uncertainty in carbon emissions from land-use change (ELUC). We develop a new oil palm plant functional type (PFT) using the JULES land surface model, called JULES-Palm. This PFT incorporates oil palm-specific physiological, structural and plantation-management traits, including rotation-based harvest/replanting cycles, and is parameterised from literature-derived values before calibration using eddy covariance (EC) and allometric observations, including leaf area index (LAI), above-ground biomass and canopy height. This calibration improves simulated photosynthesis and the vegetation structure. We then ran JULES-Palm to quantify the contribution of oil palm plantations to Indonesian ELUC, using land-use drivers from the Mapbiomas Indonesia 2.0 land cover maps (2000-

https://doi.org/10.5194/egusphere-2026-3689
Preprint. Discussion started: 28 July 2026

2022). We investigated three scenarios: (i) oil palm represented as a generic crop, (ii) oil palm omitted and treated as natural vegetation and (iii) explicit oil palm PFT. The mean and interannual variability of Indonesian ELUC (without peat emissions) is 0.058 ± 0.012 PgC_yr^{-1} with the oil palm PFT and 0.052 ± 0.010 PgC_yr^{-1} when oil palm is omitted; representing oil palm as a generic cropland gives 0.066 ± 0.011 PgC_yr^{-1}. Cumulatively, the expansion of oil palm plantations by 10.5 Mha since 2000 contributed approximately 0.14 PgC, accounting for 10.3% of Indonesia's total ELUC including legacy fluxes, but approximately 89% of land-use change attributable to conversions occurring during 2000-2022. Representing oil palm as a dedicated PFT reduces the estimated oil-palm-related ELUC relative to the generic-cropland representation by capturing plantation-specific biomass accumulation and carbon turnover. Thus, using a specific PFT for oil palm is preferable to providing a more accurate, process-based representation of plantation carbon dynamics, but treating oil palm as cropland still captures a first-order estimation of ELUC when a dedicated PFT is unavailable.

1 Introduction

Oil palm (*Elaeis guineensis*) plays a central role in the economy and land-use dynamics of equatorial Asia. Over the past few decades, the global demand for palm oil has grown rapidly due to its diverse applications in food, cosmetics and bioenergy products, making it one of the most traded vegetable oils worldwide (Murphy et al., 2021; Qaim et al., 2025). Indonesia and Malaysia are the key producers of the palm oil sector, accounting for >80% of total global production, with about 43-47 million (Indonesia) and 19-20 million (Malaysia) metric tons of crude palm oil produced per year (Rittgers et al., 2019; Shigetomi et al., 2020; UNDP, 2020; USDA, 2025). The area devoted to oil palm cultivation now exceeds 22 million hectares across both countries (Danylo et al., 2021), transforming vast landscapes that were once covered by tropical forests into monoculture plantations. This result makes oil palms a major contributor to rapid regional land-use change and carbon emissions (Carlson et al., 2012; Friedlingstein et al., 2026; Harris et al., 2021; Vijay et al., 2016).

The growth of oil palm plantations is closely associated with deforestation, peatland conversion, and degradation of natural ecosystems (Cooper et al., 2020; Koh et al., 2021; Ramdani and Hino, 2013). In Indonesia, oil palm expansion has been responsible for an estimated 23% of total forest loss (Austin et al., 2019; Lim et al., 2024). Between 2001 and 2019, around 3.09 million hectares of old-growth forests were converted into oil palm plantations, comprising about 2.13 million hectares developed as industrial-scale estates and 0.72 million hectares managed by smallholders (Gaveau et al., 2022). A similar pattern has been reported across Malaysia (Miettinen et al., 2016). These land-use changes have substantial implications for carbon emissions and ecosystem functions, particularly because many of these areas were previously carbon-dense tropical forests or peatlands (Clough et al., 2016; Guillaume et al., 2018).

At the same time, the physiological and ecological characteristics of oil palm are highly distinct from other crops and forest types typically represented in land surface models. Oil palm is a perennial monocot with a solitary columnar stem and a sequential series of phytomers produced from the apical meristem, with each phytomer bearing a leaf and an associated inflorescence or fruit bunch (Fan et al., 2015; Lewis et al., 2020; Xu et al., 2021). Each phytomer follows a well-defined life

https://doi.org/10.5194/egusphere-2026-3689
Preprint. Discussion started: 28 July 2026

cycle that includes leaf initiation, inflorescence development, fruit maturation, and pruning (Xu et al., 2021). Mature palms can sustain ~40 visible expanded phytomers, with new ones produced at approximately 20-24/year, or about 2 per month (Corley and Tinker, 2016; Fan et al., 2015). The canopy structure, photosynthetic activity, and carbon allocation processes of oil palm are thus markedly different from those of both tropical forests and annual croplands (Lewis et al., 2020). These unique characteristics influence evapotranspiration (Röll et al., 2019), surface albedo (Sabajo et al., 2017), carbon uptake (Meijide et al., 2020), plant and soil carbon turnover (Guillaume et al., 2018), making the direct substitution of oil palm with generic tropical or cropland plant functional types (PFTs) inadequate (Fan et al., 2015; Xu et al., 2021).

However, despite oil palm's significant contribution to regional and global carbon fluxes, it remains poorly represented in most global and regional models. The majority of dynamic global vegetation models (DGVMs) and Land Surface Models (LSMs) – including those used in Earth System Models (ESMs) – represent vegetation through a discrete set of generic PFTs (Sitch et al., 2015). In these frameworks, oil palm is often classified as cropland (Brasika et al., 2025). This generalisation neglects the unique morphology, phenology, and management cycle of oil palm, such as continuous fruiting, shallow root systems, and regular pruning and harvesting practices (Carlson et al., 2012). As a result, estimates of carbon emissions and land-use change impact in palm-dominated regions remain highly uncertain (Fan et al., 2015; Xu et al., 2021).

Several studies have recently addressed this gap by introducing oil palm-specific representations in global models. The CLM-Palm model (Fan et al., 2015) developed a sub-canopy and sub-PFT framework to simulate phytomer-level processes, while the ORCHIDEE-MICT-OP model (Xu et al., 2021) incorporated age-dependent phenology and carbon allocation to represent oil palm growth and management cycles. These developments have substantially improved the realism of carbon, water and energy flux simulations in palm systems (Fan et al., 2019). However, these approaches are relatively detailed and closely linked to the structural design of their respective host models. A complementary approach is therefore needed for land-surface models, in which oil palm expansion must be represented consistently in large-scale land-use change simulations without requiring major restructuring of vegetation dynamics.

Here, we develop JULES-Palm as a scalable, PFT-based representation of managed oil palm plantations within the Joint UK Land Environment Simulator (JULES). Rather than resolving phytomer-level architecture or detailed age-cohort dynamics, JULES-Palm introduces palm-specific physiological and structural traits into the existing JULES-TRIFFID framework, together with plantation establishment, replanting cycles and productivity dynamics consistent with field observations in Southeast Asia. This provides a third, more generic approach to representing oil palm in Earth-system land-surface modelling and enables an explicit assessment of how the expansion of oil palm plantations affects land-use change emissions.

https://doi.org/10.5194/egusphere-2026-3689
Preprint. Discussion started: 28 July 2026

2 Methods

2.1 JULES-Palm model development & experimental design

2.1.1 JULES-Palm structure & parameterisation

JULES is a community land surface model that can operate either in stand-alone mode or as the land surface component of the UK Met Office Earth system model (UKESM). Its structure and processes are detailed in Best et al., (2011), Burton et al., (2019), Clark et al., (2011), Littleton et al., (2020), and Wiltshire et al., (2021). JULES simulates surface energy, carbon, and water fluxes on sub-daily time steps. For each plant functional type (PFT), gross primary productivity (GPP) and net primary productivity (NPP) are accumulated and subsequently used by TRIFFID – the dynamic global vegetation model within JULES – to update vegetation structure and coverage. We set TRIFFID (Cox, 2001) to update daily, separating NPP into contributions from increasing LAI and canopy height for growth, and from expanding PFT area within the grid cell. There is spatial competition based on height, in which taller PFTs first take over spatial availability, while sustaining growth by providing sufficient NPP (Clark et al., 2011).

We employ TRIFFID-crop (Cox, 2001; Littleton et al., 2020), which extends the standard vegetation framework to represent managed agricultural systems within the carbon-climate coupling. This module represents multiple agricultural land classes – food crops, pasture and bioenergy – each occupying user-defined, temporally variable fractions of a grid cell. Within TRIFFID-crop, PFTs compete only with other PFTs belonging to the same land class through height-based dynamics, while unoccupied fractions default to bare soil (Harper et al., 2018). Identically parameterised PFTs may occur across multiple land classes (e.g. C3 grass in natural, crop and pasture areas).

As JULES lacks an oil palm PFT, we are developing one to properly represent oil palm plantations in carbon cycling. This is developed based on an improved tropical broadleaf evergreen PFT, which has been expanded beyond the original five PFTs in the previous JULES version (Harper et al., 2016, 2018). Oil palm shares key traits with managed broadleaf evergreen trees, including a perennial canopy, high LAI and continuous carbon turnover. Thus, our oil palm PFT builds on the tropical evergreen framework and follows approaches adopted in other DGVMs (Fan et al., 2015; Xu et al., 2021), while introducing palm-specific physiological traits.

However, as oil palm has distinct physiological and structural traits, we use several field observations and experimental measurements of oil palm (Agus et al., 2013; Ali et al., 2021; Cheah and Teh, 2020; Dufrene and Saugier, 1993; Fan et al., 2015; Intara et al., 2018; Perez et al., 2022; de Vos et al., 2023), including photosynthesis temperature response, stomatal conductance and canopy properties. To address limitations in the available dataset for some parameters, we also utilise values from the JULES broadleaf evergreen tree tropical (BETr) PFT, which were then calibrated using sensitivity experiments.

https://doi.org/10.5194/egusphere-2026-3689
Preprint. Discussion started: 28 July 2026

2.1.2 Palm-specific physiological parameter adjustment

Several parameters were set to reflect the differences between oil palm and BETr PFT. These are adjusted based on available published literature on leaf-level, canopy-scale, and eco-physiological observations; these values serve as a baseline before calibration.

Oil palm exhibits lower temperature sensitivity of photosynthetic capacity than many woody tropical trees, with frond photosynthesis remaining efficient under high daytime temperatures (Dufrene and Saugier, 1993). Accordingly, the activation energies for photosynthetic capacity were reduced relative to the default tropical broadleaf evergreen tree (BETr) values (act_jmax = 32,810 Jmol^{-1}; act_vcmax = 57,550 Jmol^{-1}, compared with BETr values of 64,000 and 86,900 J mol^{-1}, respectively (Oliver et al., 2022)), consistent with leaf-level measurements reported by Cheah and Teh, (2020). Physiological studies further indicate that oil palm can sustain high photosynthesis and gas exchange rates across a range of warm conditions (Bayona-Rodriguez and Romero, 2019) and that key photosynthetic capacity traits differ from other plant functional types (Ali et al., 2021).

To represent the high thermal tolerance of oil palm photosynthesis, deactivation energies were increased (deact_jmax = 443,600 J mol^{-1}; deact_vcmax = 500,000 J mol^{-1}) (Cheah and Teh, 2020), reflecting the persistence of photosynthetic activity at elevated temperatures observed in plantation systems. As oil palm has a broader thermal optimum, the entropy terms are adjusted (ds_jmax = 1400; ds_vcmax = 485) relative to the BETr defaults (646 and 649, respectively). This value controls the curvature temperature response function and is consistent with tropical monocot physiology (Cheah and Teh, 2020; Salvucci and Crafts-Brandner, 2004).

Based on reported Jmax/Vcmax ratios of oil palm fronds (Cheah and Teh, 2020; Perez et al., 2022), the ratio of electron transport needs to be reduced (jv25_ratio = 1.25, compared with 1.6 for BETr). Then the measurements of canopy light-use efficiency and leaf nitrogen-photosynthesis of oil palm (Ali et al., 2021; Dufrene and Saugier, 1993) were used to set the canopy quantum efficiency (alpha_io = 0.051) and nitrogen-use efficiency (neff_io = 0.0034).

As palm has a dense crown, the light extinction coefficient needs to be set to kext_io = 0.4, consistent with measured light attenuation profiles (Breure, 2024). The thick and long-lived frond of oil palm is also represented by increasing lma_io = 0.14 (Ali et al., 2021). Growth respiration costs were increased (r_grow_io = 0.35) following values used in other oil palm modelling studies (Xu et al., 2021). This setting reflects palm morphology.

Finally, thermal tolerance limits were modified to reflect oil palm's adaptation to the equatorial climate. The lower temperature threshold for growth was reduced (tlow_io = 0 °C) to avoid artificial cold limitation in tropical environments where oil palm is never exposed to frost (Corley and Tinker, 2016). As oil palm photosynthesis remains active at high temperature (Cheah and Teh, 2020) with suitable temperature 19-35 °C (Zhao et al., 2024) and leaf temperature in tropical canopies can frequently exceed 45 °C (Rey-Sánchez et al., 2016), we need to increase the upper temperature limit (tupp_io = 50 °C).

These adjusted PFT parameters provide a realistic starting point for representing oil palm PFTs. The final PFT parameters will be set after calibration using Latin Hypercube Sampling (LHS), as described in section 2.4.

https://doi.org/10.5194/egusphere-2026-3689
Preprint. Discussion started: 28 July 2026

2.1.3 Plantation management representation

Oil palm was assigned to the bioenergy land class within JULES-BE (Littleton et al., 2020), which represents managed perennial vegetation and allows the application of rotation-based management while retaining dynamic vegetation processes. This land-class choice reflects the plantation nature of oil palm and distinguishes it from both natural forest vegetation and annual cropland.

To approximate the shallow rooting system characteristic of oil palm, we prescribed a reduced effective rooting depth to 0.5 m (Intara et al., 2018; Nelson et al., 2006). This setting concentrates the water uptake in the upper soil layers while still allowing limited access to deeper moisture in the default exponential root distribution.

We use our observations of LAI across sites in Southeast Asia (Figure 3) to accurately reflect oil palm LAI development throughout the plantation lifecycle. The lower set represents juvenile plantations, which typically include at least 1-year-old trees, while the upper bound corresponds to the observed range of mature oil palm canopies (Table 1).

2.1.4 Assisted Expansion

In TRIFFID-crop, newly expanded agricultural land is, by default, initialised as bare soil and subsequently colonised by vegetation spread according to productivity and biomass. While appropriate for natural vegetation, this behaviour is less representative of managed agricultural systems, where expansion typically involves active planting.

To better reflect plantation establishment, we activated the existing assisted expansion option (Table 1). Under this setting, when the fractional area of an agricultural land class increases, newly added area is directly assigned to eligible PFTs within that land class rather than remaining bare soil. For oil palm, this ensures it aligns with real-world planting practices that use young oil palm trees.

2.1.5 Harvest representation for oil palm

Our harvest setting reflects oil palm as a managed perennial PFT; we set periodic harvests to represent plantation replanting rather than annual fruit harvesting. A harvest frequency of 25 years was prescribed, consistent with the oil palm replanting cycle in Southeast Asia. We also set the vegetation height to 1 m after harvest, as common replanting utilises young oil palm plants. Based on our observations, the juvenile period of oil palm (1-5 years old) has a canopy height of around 0.2-1.5 m. This periodic harvesting should realistically reflect the renewal of the oil palm plantation.

This configuration does not represent routine FFB harvesting. In real plantations, FFB harvest removes reproductive biomass repeatedly during the plantation lifetime, without reducing canopy height or removing the long-lived structural biomass of stems, leaves and roots. Reported FFB productivity varies substantially among plantations, but mature oil palm can produce more than 10 t FFB ha^{-1} yr^{-1}, with high-yielding mature plantations reaching approximately 30 t FFB ha^{-1} yr^{-1} (Siang et al., 2022; Teh and Sung, 2016; Zolfagharnassab et al., 2022). Recent studies have converted annual oil palm fruit bunch production

https://doi.org/10.5194/egusphere-2026-3689
Preprint. Discussion started: 28 July 2026

to carbon using a dry-matter fraction of 0.50 and a carbon fraction of 0.557 (Wakhid et al., 2022; Wakhid and Hirano, 2021). These values indicate that FFB harvest can represent a substantial annual carbon export from the plantation.

In the current JULES-Palm configuration, however, there is no separate fruit or reproductive carbon pool and no repeated FFB product-export flux. Carbon allocated to reproductive tissues is therefore not explicitly removed as harvested product. Instead, the model carbon balance reflects vegetation growth, turnover, litter input, soil decomposition and the periodic stand-replacement harvest. Consequently, the simulations are designed to assess carbon-stock changes associated with land-use conversion, plantation regrowth and replanting, rather than the full plantation product-export carbon cycle. We therefore treat missing FFB-C export as a model limitation and assess its potential magnitude using a first-order diagnostic in the Discussion (Table 3), but we do not apply it as a direct correction to ELUC. The detailed JULES-Palm settings are shown in Table 1.

Table 1 JULES-Palm configuration used to represent oil palm plantation establishment, rooting depth, canopy development, assisted expansion, and replanting management.

Process represented	JULES option/parameter	Value	Interpretation
Land-class assignment	Bioenergy land class	Oil palm assigned to bioenergy land class	Represents oil palm as managed perennial vegetaion rather than natural forest or annual crop
Rooting depth	rootd_ft_io	0.5 m	Reduces effective rooting depth to reflect the shallow rooting distribution of oil palm
Soil moisture stress/ root distribution option	fsmc_mod_io	0	Retains the default exponential root distribution used for soil moisture uptake
Minimum leaf area index	lai_min_io	0.27 m^2 m^{-2}	Represents low canopy leaf area during young plantation establishment
Maximum leaf area index	lai_max_io	7.0 m^2 m^{-2}	Constrains mature oil palm canopy LAI to observed values from Southeast Asian sites
Assisted agricultural expansion	l_ag_expand	.true.	Newly expanded agricultural area is actively assigned to eligible PFTs instead of first appearing as bare soil
Harvest type	harvest_type_io	2	Represents periodic stand-replacement harvest/replanting rather than annual fruit harvest
Harvest frequency	harvest_freq_io	25 years	Represents a typical oil palm replanting cycle
Post-harvest vegetation height	harvest_ht_io	1.0 m	Represents young palms after replanting

https://doi.org/10.5194/egusphere-2026-3689
Preprint. Discussion started: 28 July 2026

2.2 The forcing dataset

2.2.1 Land-use change dataset (Mapbiomas Indonesia)

Mapbiomas Indonesia is a LULCC (Land Use and Land Cover Change) dataset that utilises Landsat imagery and employs a pixel-based approach, combined with a machine learning algorithm, to analyse it, leveraging the powerful cloud-processing capabilities of Google Earth Engine (GEE). This is adapted from *Mapbiomas Brazil, which* started in 2015, with some adjustments for local/national uniqueness (MapBiomas, 2023).

For example, *Mapbiomas Indonesia* has specific categories of Oil Palm. This is because oil palm makes a major contribution to land-use changes in Indonesia, accounting for 58- 60% of world palm oil production (Dermoredjo et al., 2025; Shigetomi et al., 2020; USDA, 2025). Apart from Oil Palm, agriculture in *Mapbiomas Indonesia* 2.0 (MB2) is also categorised as rice paddy, pulpwood plantation, and other agriculture – which in JULES we treat as a single crop type, irrigated and with the same physiology as grassland.

MB2 has a high spatial resolution of 30 meters, enabling it to detect even small changes in LULCC (Mapbiomas Indonesia, 2022). We resample this dataset as a land fraction of 0.5° to make it compatible with JULES. This dataset is widely used for various research, including the calculation of CO_2 emissions from land-use change (Brasika et al., 2025; Friedlingstein et al., 2023, 2026). MB2 cover the whole area of Indonesia from 2000 to 2022.

2.2.2 Land use scenarios for JULES-Palm

In this study, the annual MB2 (Fig. 1) is used across 3 land cover scenarios (Fig. 2) to quantify the effect of oil palm representation on estimates of carbon emissions from land-use change (ELUC). The ELUC is highly affected by the conversion of forested areas to other land uses, primarily agricultural uses. This agriculture might consist of cropland, grazing land or other agriculture such as oil palm.

https://doi.org/10.5194/egusphere-2026-3689
Preprint. Discussion started: 28 July 2026

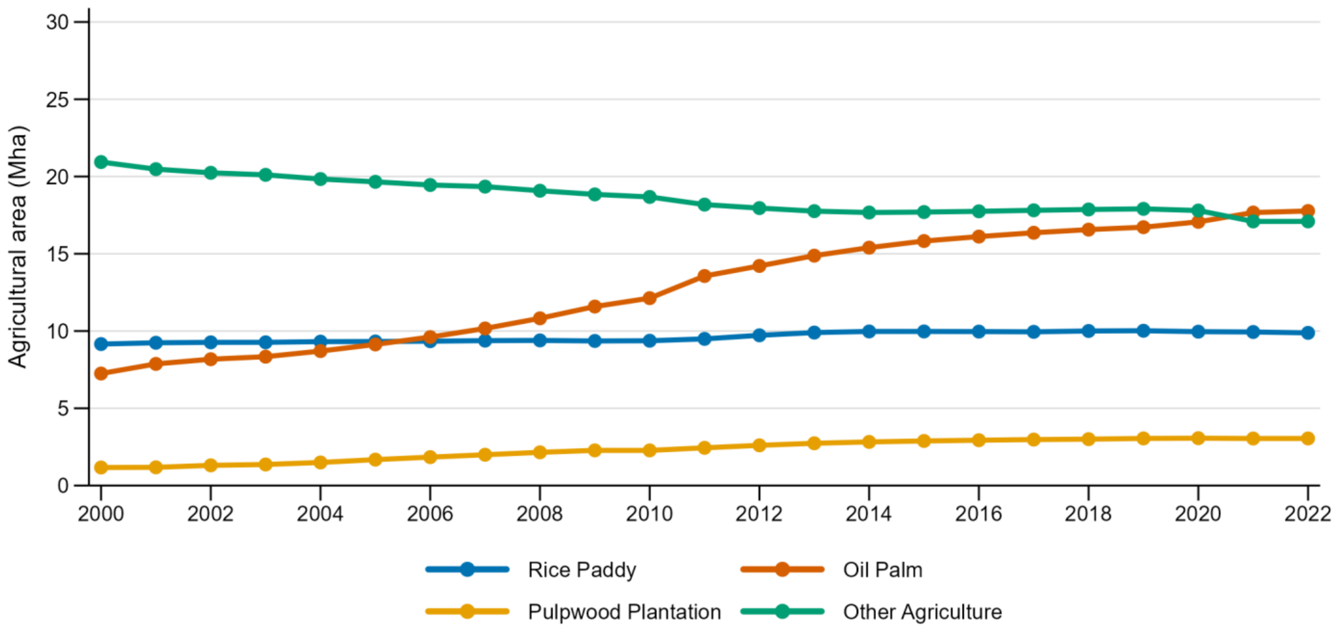

Figure 1: Timeseries of agricultural land use in MB2 dataset from 2000 to 2022 used as forcing in the JULES-Palm model. Data from Mapbiomas Indonesia (2022).

In the first scenario, we define oil palm as a generic cropland (together with paddy and other croplands), similar to models in the Global Carbon Budget (GCB) (Friedlingstein et al., 2023, 2025). This scenario is necessary to avoid neglecting oil palm's contribution. As many models lack an oil palm PFT (plant functional type) in their systems, this approach addresses it. The second scenario excludes LUC for oil palm; in this scenario, oil palm plantations are not represented in any land use, not in cropland or other land use, but are classified as natural vegetation. This scenario simulates ELUC in the absence of oil palm plantations, allowing us to understand the contribution of oil palm plantations to total ELUC. The third scenario introduces a new PFT, Oil Palm. In this last scenario, we examine our new PFT of oil palm to represent land-use change caused by oil palm plantations.

https://doi.org/10.5194/egusphere-2026-3689
Preprint. Discussion started: 28 July 2026

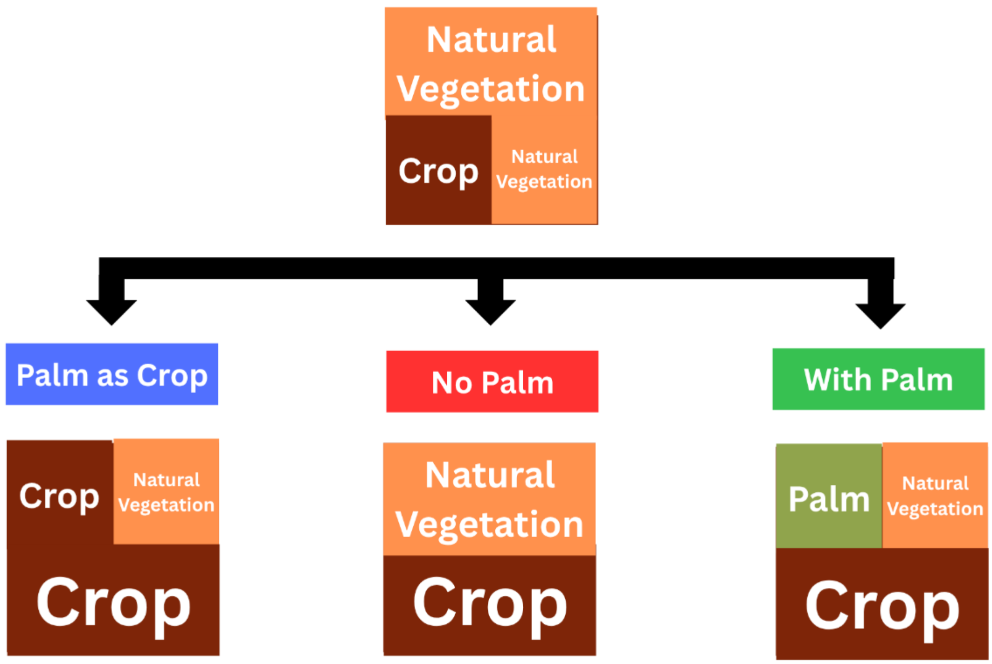

Figure 2: The three LULCC scenarios applied in the JULES-Palm simulation to estimate oil palm effect on carbon emissions. Scenario 1 (left), Scenario 2 (middle) and Scenario 3 (right)

Scenario 3 minus Scenario 2 gives the ELUC contribution from oil palm expansion, while Scenario 3 minus Scenario 1 estimates the difference in ELUC estimate when representing oil palm as a specific crop rather than a generic crop. In all three scenarios, we used the same pasture dataset, adjusted according to the first scenario. If the total land fraction of cropland (including oil palm) and pasture exceeds 1, we reduce pasture to a maximum of 1 (i.e., 100% grid cell cover). We use this pasture for other scenarios, with and without palm plantation. We distinguish between total ELUC over 2000-2022 and ELUC attributable to land-use transitions occurring within 2000-2022. Total ELUC includes legacy fluxes, defined here as ongoing carbon fluxes during 2000-2022 arising from land-use changes that occurred before the analysis period. These fluxes occur because vegetation, litter and soil carbon pools continue to adjust after a land-use transition. Therefore, Scenario 3 minus Scenario 2 represents the total effect of representing oil palm expansion, including both contemporary oil palm transitions during 2000-2022 and any legacy carbon-pool adjustments present during the simulation period. To isolate emissions from contemporary oil palm expansion, we additionally calculated ELUC using only fluxes associated with land-use transitions prescribed during 2000-2022.

2.3 Oil palm observations datasets

We use the eddy covariance (EC) tower dataset as observations to evaluate JULES simulations. In addition to the EC fluxes that represent net ecosystem CO_2 exchange in oil palm plantations and derived quantities such as GPP, we also collect several datasets of oil palm allometries to adjust JULES PFT settings, including leaf area index (LAI), above-ground biomass (AGB), and canopy height. For the spatial analysis, we utilise oil palm spatio-temporal change from Mapbiomas Indonesia 2.0 (Mapbiomas Indonesia, 2022) as a driver forcing, following the same protocol as in GCB (Friedlingstein et al., 2023, 2026).

2.3.1 Eddy covariance at oil palm

The EC towers are located in commercially managed oil palm plantations situated in Sabaju (3°9.615'N,113°25.163'E) and Sebungan (3°9.965'N,113°21.198'E) in Sarawak, northern Borneo (McCalmont et al., 2021) with a 20 m high tower (see figure 3). These towers are 7.3 km apart. The sites were established on deep peat (up to 8 m) in the region and previously logged Peat Swamp Forest (PSF) cleared and drained by cutting a regular network of drainage channels prior to palm establishment (Cook et al., 2018).

The previously degraded forest at Sabaju was cleared (without burning) at the beginning of 2016, with forest biomass cut and compacted on site and drainage channels cut into the peat. Establishment of oil palm (~160 plants/ha) was completed by the end of April 2016 and followed commercial practice throughout; no harvest was taken from the immature palms during the study period. The Sebungan plantation was established in July 2007, with fruit bunch harvesting starting from month 32.

In our simulation validation, we use the GPP from the EC dataset for the entire 2017-2019 period in Sabaju and for the 2018 period in Sebungan (McCalmont et al., 2021). This represents young oil palm (1-3 years old) in Sabaju and mature oil palm (~10 years old) in Sebungan, thereby providing information on oil palm plantation dynamics. The dataset is available at 30-minute intervals and is gap-filled.

2.3.2 Oil palm allometric database

We complemented the EC flux dataset with a compilation of oil palm allometric observations. Studies include field measurements across Southeast Asia – Indonesia, Malaysia and Thailand – where the same species and broadly similar management practices prevail. LAI was our primary structural variable because JULES uses LAI to determine AGB and canopy height (canht), see equations 1 and 2. We assembled LAI observations spanning plantation ages and fitted an exponential age-LAI relationship, which was used to drive the model's allometric equations (Awal et al., 2010; Fan et al., 2015).

In the context of carbon emissions, we focused on AGB and canopy height as key indicators of carbon storage. The AGB database comprises 47 site-age observations from Bukit Dua Belas, Genting, Harapan, Sabaju, Sebungan, South Sulawesi, Teluk Intan and West Malaysia with long time series available at Genting and Teluk Intan (Fan et al., 2015; Ida Sunaryathy et al., 2015; Kotowska et al., 2015; Teh and Sung, 2016; Xu et al., 2021). The canopy height dataset includes 29 observations

https://doi.org/10.5194/egusphere-2026-3689
Preprint. Discussion started: 28 July 2026

from Banh Saphan Noi (Thailand) and South Malaysia (Kluang, Genting and Sime Darby) (Kulpanich et al., 2022; Tan et al., 2014) (Figure 3).

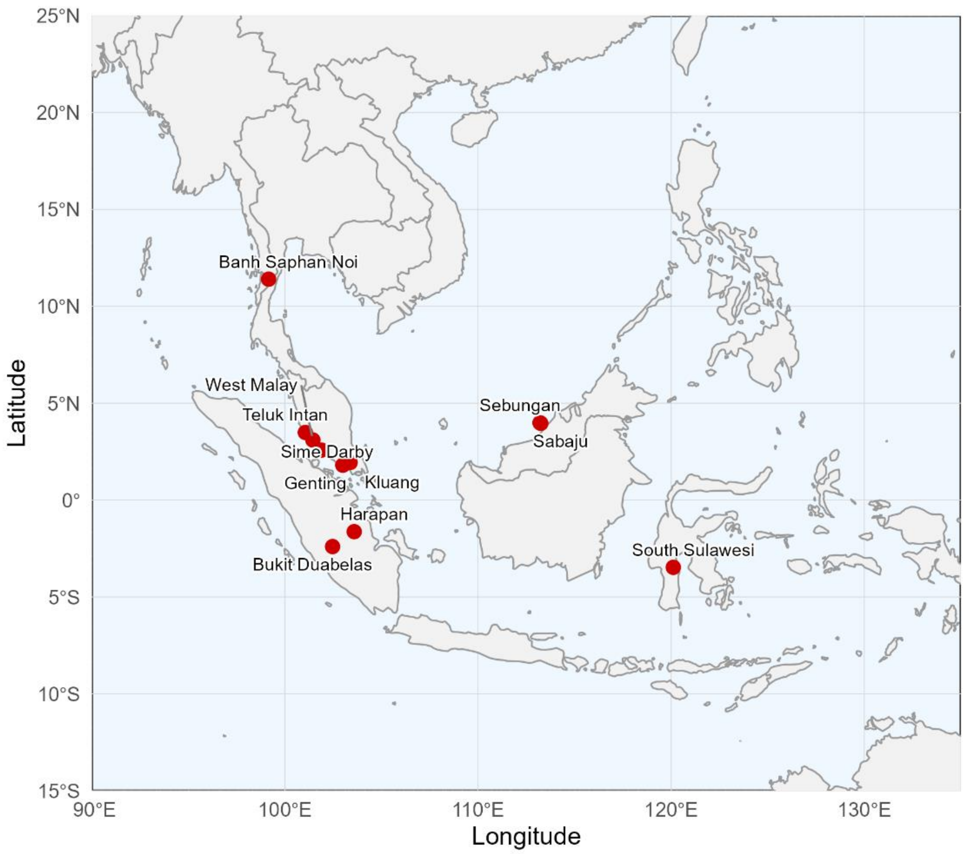

Figure 3: Location of observation sites used for JULES-Palm calibration of Oil Palm in Southeast Asia

In JULES, the AGB (equation 1) and canopy height (equation 2) are defined as follows:

$$AGB = a\_wl * LAI^{b\_wl} + LAI * lma\_io * 0.4 \quad (1)$$

$$canht = \frac{a\_wl * LAI^{b\_wl-1}}{a\_ws * \eta\_sl} \quad (2)$$

Where a_wl and b_wl are empirical allometric coefficients, lma_io represents the leaf mass per area, a_ws is the stem density scaling factor, and η_sl denotes the structural efficiency coefficient.

https://doi.org/10.5194/egusphere-2026-3689
Preprint. Discussion started: 28 July 2026

2.4 Model calibration

To constrain parameter uncertainty and ensure physiologically realistic behaviour of the oil palm PFT, we calibrated the model against key observed variables governing the carbon cycle, namely GPP and vegetation structure (AGB and canopy height). We calibrated the PFT parameters that relate to photosynthetic capacity (e.g., Vcmax, Jmax), canopy radiative transfer (e.g., kext_io), and biomass allometry (e.g., a_wl, a_ws); evergreen phenology was also calibrated to reflect continuous leaf production typical of oil palm physiology.

We optimised parameters using Latin Hypercube Sampling (LHS) in two separate experiments. First, a 500-member ensemble was used to optimise photosynthesis-related parameters, each varied within ±30% of their default values. Second, a 4000-member ensemble was used to optimise allometric parameters controlling vegetation structure (AGB & canopy height), with a ±50% range. Photosynthesis parameters are relatively well constrained by physiological understanding and literature values, so were perturbed within a narrower range to maintain realistic behaviour. A larger range and ensemble size were chosen for second optimisation because these parameters are strongly coupled through non-linear relationships governing vegetation structure (see equations 1 and 2). Additionally, a preliminary evaluation showed that the simulated canopy height was approximately three times the observed value, justifying a wider exploration range. These LHS calibrations explore the PFT parameter space to find the most reliable combination that best reflects the observed oil palm physiological behaviour. Table 2 shows the PFT parameters that have been calibrated.

Table 2 Calibrated plant functional type (PFT) parameters used in JULES-Palm, compared with the default BETr values. Parameters were derived from published oil palm measurements and further optimised using LHS calibration experiments.

Parameters	BETr	JULES-Palm	Rationale
a_wl	0.845	0.55	Optimised via 4000-member LHS calibration (±50%), reducing leaf biomass density to reflect observed palm architecture and moderating early structural growth.
a_ws	13	16.14	Optimised via 4000-member LHS calibration (±50%), to match empirical stem mass accumulation rates consistent with plantation observations.
act_jmax	64000	30122	Set up via empirical data for oil palm (Cheah and Teh, 2020) which represent lower activation energy for Jmax in palm fronds. Then calibration with LHS (±30%)
act_vcmax	86900	59361	Based on leaf-level measurement by Cheah & Teh, 2020 to reflect lower temperature sensitivity of Vcmax for oil palm. Tuned up with ±30% LHS.

https://doi.org/10.5194/egusphere-2026-3689
Preprint. Discussion started: 28 July 2026

alpha_io	0.064	0.065	Based on canopy light-use efficiency measured in oil palm (Dufrene and Saugier, 1993) and refined via ±30% LHS search.
b_wl_io	1.667	1.838	Estimated via 4000 members ±50% LHS ensemble to reproduce observed nonlinear scaling of leaf biomass with canopy development.
deact_jmax	200000	500716	Adjusted based on Cheah & Teh, 2020 temperature response analysis and tuned via ±30% LHS to reflect high thermal tolerance of palm photosynthesis enzymes.
deact_vcmax	200000	499539	Assigned based on Cheah & Teh, 2020 temperature response analysis and tuned via ±30% LHS.
ds_jmax	646	1012	Based on Cheah & Teh, 2020 biochemical parameters and adjusted via ±30% LHS to capture sharper decline in palm enzymatic activity beyond optimum temperature.
ds_vcmax	649	546	Adopted C3 plant default due to limited palm-specific evidence and refined via ±30% LHS.
η_sl	0.01	0.012	Adopted from BETr, then calibrated using LHS ±50% to match structural efficiency consistent with palm frond production and crown architecture.
g1_stomata	5.31	5.98	Using stomatal slope measurement for oil palm to set up functional-structural simulation (Perez et al., 2022). Followed with calibration ±30% LHS.
gpp_st_io	1.58E-07	2.05E-07	Calibrate BETr value with ±30% LHS to align simulated GPP sensitivity with EC observations at young and mature plantations.
jv25_ratio	1.6	1.23	Based on Jmax/Vcmax ration of oil palm, reported by (Cheah and Teh, 2020; Perez et al., 2022). Followed by calibration ±30% LHS.
kext_io	0.5	0.4	Reduced to 0.4 based on measurement of light extinction coefficient in oil palm canopies (Breure, 2024); This is typical value for dense palm crowns.
lma_io	0.1036	0.198	Set from available observation of LMA in oil palm plantation by Ali et al., 2021; (SLA-to-LMA conversion from gC fractions). Then calibrate through ±30% LHS to reproduce structural allocation.

neff_io	8.00E-04	0.00242	Set higher nitrogen efficiency to reproduce palm biochemical response curves. Then calibrate ±30% LHS and constrained by empirical Jmax/Vcmax curvature behaviour.
q10_leaf_io	2	2.44	Adopt BETr thermal sensitivity with calibration ±30% LHS to match oil palm respiration and photosynthesis.
r_grow_io	0.25	0.35	Adopted from (Xu et al., 2021) to represent higher growth respiration demand in palm tissue construction.
tlow_io	13	0	Lowered to avoid artificial cold limitation in tropical simulations; this is a model configuration choice rather than a physiological tolerance threshold.
tupp_io	43	62.13	Raised via ±30% LHS during calibration to reduce excessive high-temperature limitation in tropical condition.

2.4.1 Photosynthesis calibration (GPP)

The primary calibration of the model focused on photosynthesis, as represented by GPP. GPP observations come from EC towers at the Sabaju and Sebungan oil palm plantations. The Sabaju site has a young oil palm plantation, while the Sebungan site has mature oil palm. The EC tower provides half-hourly fluxes, which need to be aggregated to a monthly total. This simplifies comparison with JULES GPP outputs.

The calibration process involved 500 model simulations employing the LHS technique to effectively explore the parameter space. Twelve PFT parameters associated with the oil palm photosynthesis process were varied within a ±30% range. These parameters included; act_jmax, act_vcmax, alpha_io, deact_jmax, deact_vcmax, ds_jmax, ds_vcmax, gpp_st_io, g1_stomata, jv25_ratio, neff_io and tupp_io.

For each simulation, modelled monthly GPP was compared with the observed GPP to evaluate performance. The parameter set yielding the lowest Mean Absolute Error (MAE) between modelled and observed GPP was selected as the optimal calibration for representing oil palm photosynthesis behaviour in JULES.

2.4.2 Allometric calibration (AGB & canopy height)

The second calibration focuses on allometric relationships of oil palm, specifically on AGB and canopy height. These two variables are critical for accurately representing the dynamics of oil palm structure, as they govern carbon partitioning and vertical development.

We prescribe LAI using an exponential best-fit curve derived from available oil palm observations in Southeast Asia (Fig. 4). This LAI-age relationship is used to ensure a realistic canopy structure during parameter calibration. However, the LAI evolves

https://doi.org/10.5194/egusphere-2026-3689
Preprint. Discussion started: 28 July 2026

dynamically in JULES-TRIFFID simulations. This allows the oil palm canopy to respond to the dynamics of climate and carbon allocation.

The allometric calibration simultaneously optimised five key PFT parameters - a_wl, b_wl, lma_io, a_ws and - which together control the scaling of AGB and canopy height with LAI in JULES. This calibration uses a joint objective function design, prioritising accurate representation of ecosystem carbon stock by reproducing chronosequences of AGB and canopy height. There are 4,000 LHS parameter combinations to explore the multidimensional parameter space. Each combination is run in JULES, then evaluated against field observations.

Data-fit term (relative error)

The primary data-fit component (equation 3) was defined as the mean relative error between modelled and observed quantities:

$$E_X = \frac{1}{N_X}\sum_{i=1}^{N_X}\frac{\left|X_i^{mod} - X_i^{obs}\right|}{X_i^{obs}} \tag{3}$$

Where X denotes either AGB or canopy height (canht), N_X is the number of observations and X_i^{mod} and X_i^{obs} are modelled and observed values, respectively. This optimises the prevention of domination from large observations.

Slope and intercept penalties

To reduce systematic bias, an additional penalty (equation 4) was applied based on linear regression between modelled and observed values:

$$P_X = \lambda_{int}|a| + \lambda_{slope}|b-1| \tag{4}$$

Where a and b are the intercept and slope the regression $X^{mod} = a + bX^{obs}$, and λ_{int} and λ_{slope} control the strength of the penalty. This term favours solutions approaching a 1:1 relationship (slope ≈ 1, intercept ≈ 0).

Asymmetric error weighting

To avoid systematic underestimation of biomass and canopy height – particularly important for carbon stock estimation – relative errors were weighted asymmetrically (equation 5):

$$E_X^* = \frac{1}{N_X}\sum_{i=1}^{N_X}\omega_i\frac{\left|X_i^{mod} - X_i^{obs}\right|}{X_i^{obs}} \tag{5}$$

Where $\omega_i > 1$ when $X_i^{mod} < X_i^{obs}$ and $\omega_i = 1$ otherwise. This asymmetry reflects the greater importance of avoiding underestimation of carbon stocks in mature oil palm plantations.

Prior constraints.

Weak prior constraints were imposed to maintain physically and ecologically plausible parameter combinations. A constraint was applied to the product of the height-scaling parameters (aws x ηsl) (equation 6) to preserve a realistic canopy height scale:

$$P_{scale} = \lambda_{scale}\left[ln\left(\frac{a\_ws * \eta\_sl}{(a\_ws * \eta\_sl)_{target}}\right)\right]^2 \tag{6}$$

https://doi.org/10.5194/egusphere-2026-3689
Preprint. Discussion started: 28 July 2026

In addition, individual priors (equation 7) were applied to prevent unphysical deviations from empirically supported baseline values:

$$P_\theta = \sum_k \lambda_k \left(\theta_k - \theta_{k,target}\right)^2 \quad (7)$$

The θ_k represent the constrained parameters and λ_k their respective prior strengths. We use log-space for positive scale parameters, while linear prior is applied where appropriate.

Then the overall function (equation 8) is:

$$Loss = 0.6(E^*_{AGB} + P_{AGB}) + 0.4(E^*_{HGT} + P_{HGT}) + P_{scale} + P_\theta \quad (8)$$

Where the weights the objective function (data-fit & bias penalties) were normalised to sum to one, with greater emphasis placed on AGB to reflect its central role in determining ecosystem carbon stocks and land-use change emissions.

We develop these functions to meet the study objective of quantifying land-use change emissions but the structure of the function follows common practice in ecological and land surface model calibration, such as data-fit terms, bias penalties and prior constraints to balance realism and robustness (e.g. Bloom & Williams, 2015; Van Oijen, 2005; Williams et al., 2009).

3 Results

3.1 Calibration and evaluation of oil palm canopy structure and productivity

In the calibration, we use an empirical LAI-age curve to constrain oil palm canopy development (Fig. 4). LAI shows a rapid early expansion and stabilisation at the mature oil palm stage, which is consistent with realistic development timing. In subsequent simulations, LAI evolves dynamically through TRIFFID-PFT processes rather than being prescribed.

https://doi.org/10.5194/egusphere-2026-3689
Preprint. Discussion started: 28 July 2026

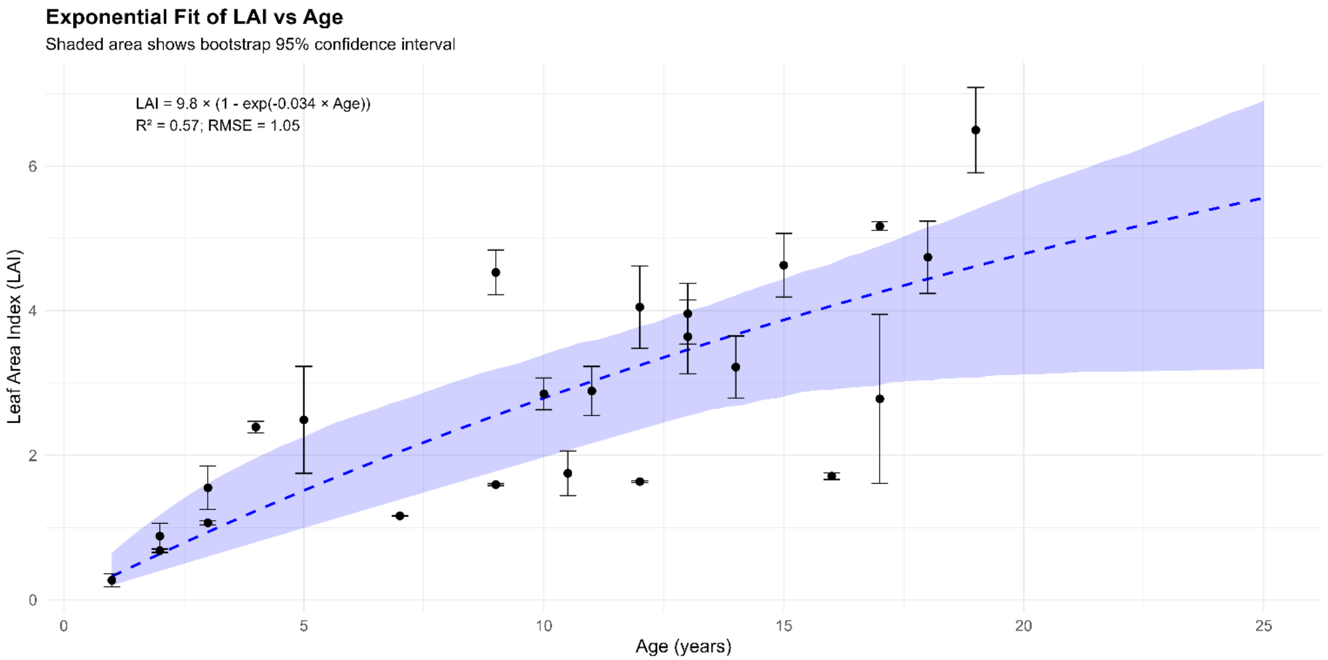

Figure 4: Best-fit relationship between LAI and oil palm age, showing the exponential regression

The calibration process substantially improved JULES performance for oil palm photosynthesis and structural growth. Figures 4-6 compare model output against observations from EC towers and plantation biomass inventories, for both the default JULES broadleaf evergreen configuration and the calibrated oil palm configuration.

Monthly GPP from JULES showed clear age-dependent behaviour relative to observations (Fig 5). At the young oil palm plantation site (1-3 years), the default JULES run slightly underestimated GPP, but the calibrated JULES-Palm closely aligned with the 1:1 line. This indicates the accurate simulation of oil palm photosynthesis during the juvenile phase. Meanwhile, in Sebungan, in mature oil palm (~10 years), calibration improves the model by reducing bias, but it still underestimates GPP. This remaining underestimation may reflect the use of a single fixed oil palm PFT parameterisation for both young and mature plantations, which may not fully capture age-related changes in canopy structure, photosynthesis capacity, and stomatal behaviour. Thus, while the calibration has successfully captured photosynthesis in young oil palm, further improvements may be required to reproduce productivity in mature oil palm.

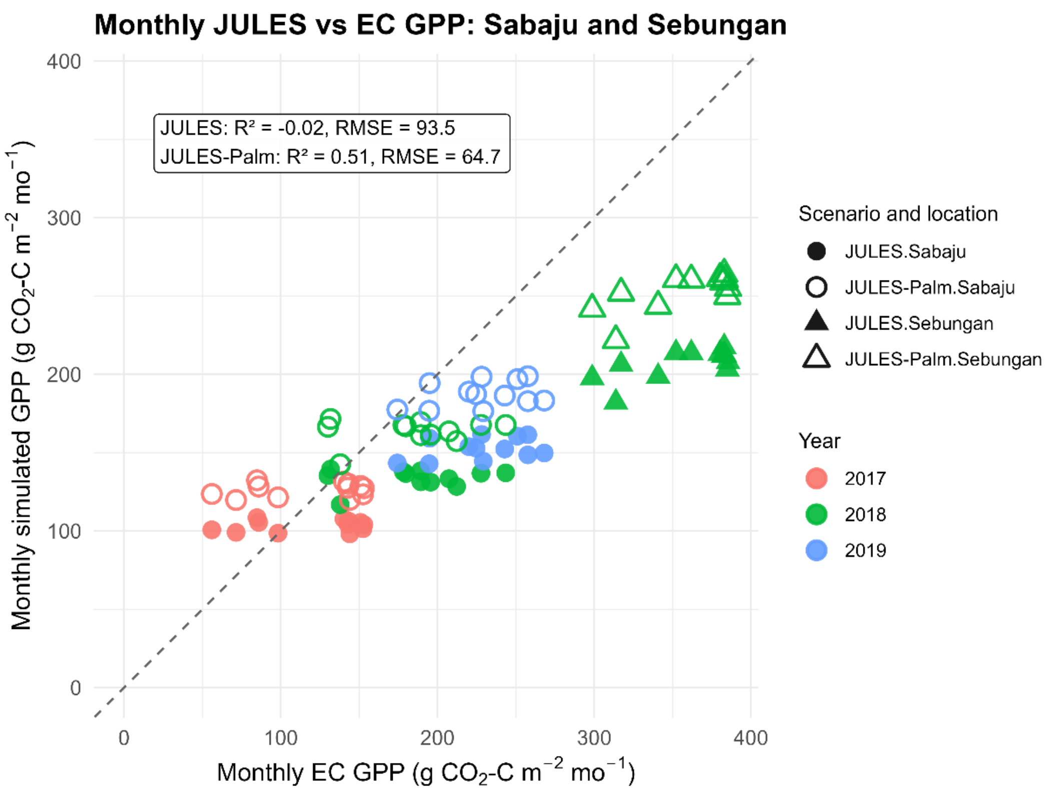

Figure 5: Scatterplot comparing monthly GPP from the JULES models and EC observation at Sabaju (young palm oil) and Sebungan (mature palm oil). Results are shown for the default JULES-ES configuration and the JULES-Palm parameterisation using LHS.

Default JULES values produced strong overestimation of AGB, exceeding observations by up to ~30-40% across the plantation chronosequence (Fig 6, panel left). In contrast, JULES-Palm show significant improvement, with the rotation period between the two sites, Genting and Teluk Intan. This improvement is clearly seen in mid- to late-rotation ages (8-20 years). A scatter plot comparison across all sites (Fig 6, right panel) confirms that JULES-Palm reduces bias and brings model estimates closer to the 1:1 relationship.

https://doi.org/10.5194/egusphere-2026-3689
Preprint. Discussion started: 28 July 2026

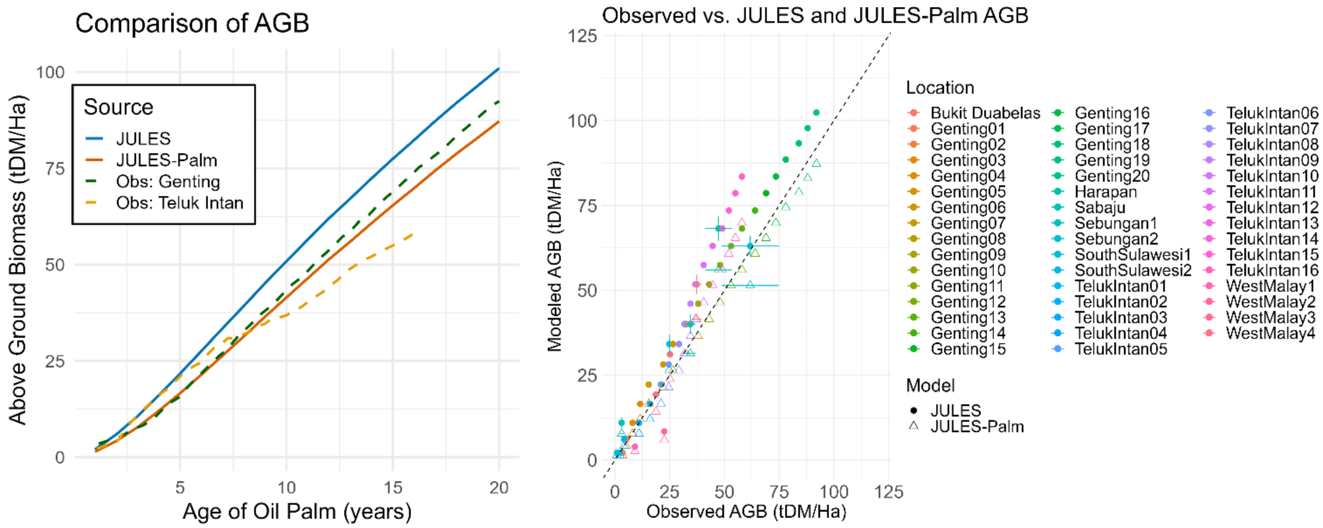

Figure 6: Comparison of AGB between model simulations and observations for oil palm. The timeseries (left) shows the development of AGB with oil palm age, comparing model simulations with observations from Genting and Teluk Intan. The scatterplot (right) compares modelled AGB from JULES and JULES-Palm with observed AGB across multiple sites.

Default JULES results suggest a large overestimation in simulated canopy height (canht)(Fig. 7); It is 3 times taller than the observed canopy height. This is because the BETr simulates natural tree PFTs with much higher canopy, whereas oil palm has a monopodial growth structure with much shorter canopy (Fan et al., 2015; Harper et al., 2016). JULES-Palm shows significant improvement, reducing the height bias and providing more realistic height-age relationships. There is a slight overestimation, but the error is significantly lower than the default.

https://doi.org/10.5194/egusphere-2026-3689
Preprint. Discussion started: 28 July 2026

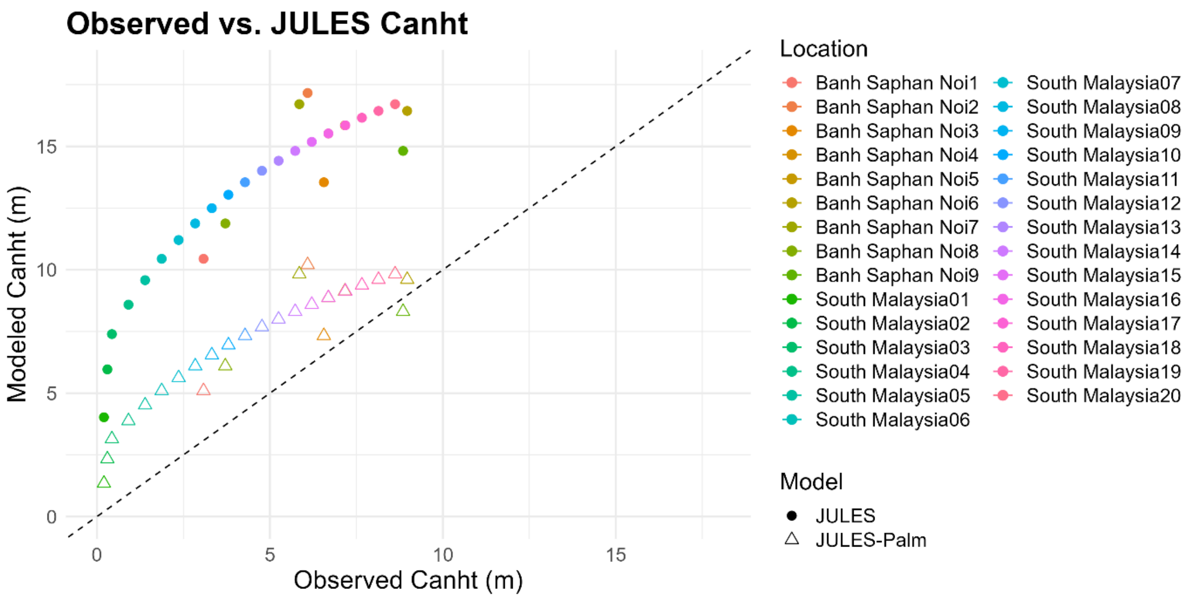

Figure 7: Scatterplot of JULES /JULES-Palm models with observed oil palm canopy height across multiple sites. "Banh Saphan Noi 1-9" denotes individual plots or site-age observations from the Banh Saphan Noi, Thailand dataset, while "South Malaysia 01-20" denotes individual observations from the South Malaysia dataset, which includes Genting, Kluang and Sime Darby records.

In general, the calibration has provided significant improvements in the representation of oil palm physiology and structure. This includes realistic photosynthesis in young oil palm, corrected height-to-biomass scaling, and improved rotation biomass accumulation.

3.2 National-scale ELUC impacts of oil palm expansions

After developing and validating the new oil palm PFT against EC and allometric observations, we applied it at the national scale to quantify the contribution of oil palm expansion to land-use change emissions (ELUC) in Indonesia (Fig 8). We prescribed oil palm land-use change from MB2 for the JULES simulations over 2000-2022.

https://doi.org/10.5194/egusphere-2026-3689
Preprint. Discussion started: 28 July 2026

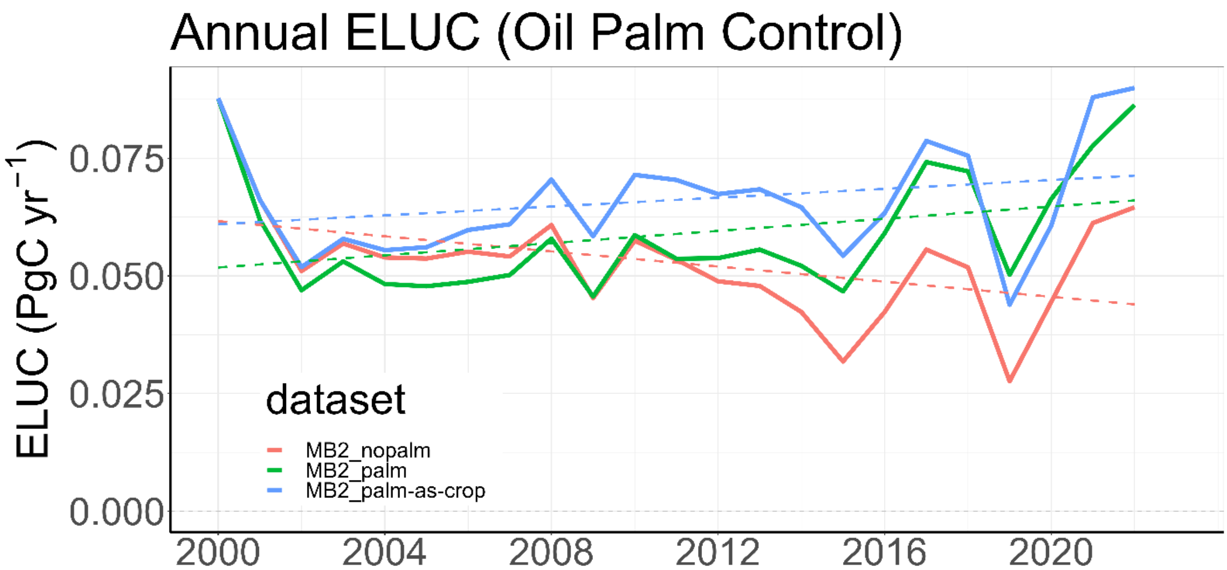

Figure 8: Annual ELUC in Indonesia from 2000-2022 under three oil palm representation scenarios

Oil palm expansion results in approximately 10.3% of Indonesia's total ELUC over 2000-2022 when legacy fluxes are included (Scenario 3 minus Scenario 2). This is equivalent to ~0.14 PgC of total cumulative carbon emissions over the study period. When the analysis is restricted to land-use change fluxes attributable to conversion occurring during 2000-2022, plantation expansion of oil palm accounts for approximately 89% of the cumulative emissions. Mean annual ELUC was 0.058 ± 0.012 PgC yr^{-1} when including oil palm as a dedicated PFT (Scenario 3), compared with 0.052 ± 0.010 PgC yr^{-1} in the simulation where oil palm land-use change was ignored (Scenario 2). The oil palm scenario, represented as generic cropland (Scenario 1), yields a larger estimate (0.066 ± 0.011 PgC yr^{-1}), ~12% higher than the dedicated oil palm PFT (Scenario 3), because generic crops have lower carbon content than oil palm trees.

The temporal evolution of ELUC also differed across scenarios. The ELUC shows a decreasing trend in the absence of oil palm scenarios, whereas simulations with oil palm show increasing emissions over time. This pattern is consistent with oil palm expansion based on the MB2 dataset. It has increased significantly by 10.5 Mha and overtaken other agricultural sectors over the past two decades. This means explicitly representing oil palm PFT has a significant impact on improving ELUC.

3.3 Process-level controls on ELUC

To diagnose why these simulations differ, we decompose ELUC into its component carbon fluxes (Fig. 9). We analyse S2-S3 differences following the TRENDY protocol (Sitch et al., 2024), where S2 represents a no land-use change control and S3 includes observed land-use transitions (Fig. 9). The value is positive if the fluxes are larger in a world without land-use change, and negative if the opposite. There are two processes that dominate the ELUC response. First, the NPP of explicit oil palm is consistently lower under the land-use change scenario, whereas S2-S3 is positive and increases through time (Fig. 9a). This means that replacing forest with oil palm plantations reduces NPP. The productivity penalty is strengthened as palm area expands nationally.

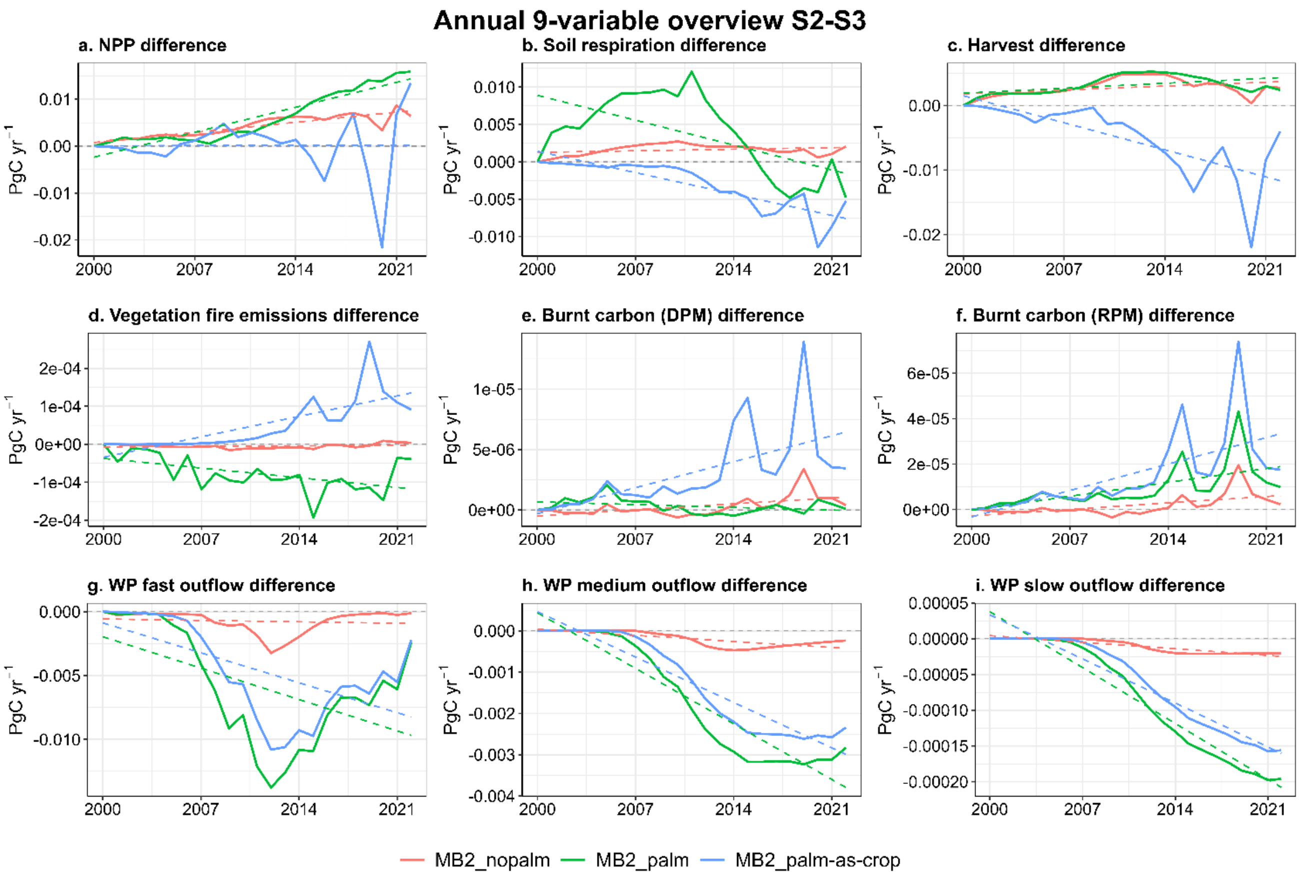

Figure 9: The differences in nine carbon-cycle components contributing to ELUC among the scenarios, which consist of: a. net primary productivity (NPP), b. soil respiration to atmosphere, c. harvest, d. vegetation fire emission, e. burnt carbon decomposable plant material (DPM), f. burnt carbon resistant plant material (RPM), g. wood products (WP) fast, h. wood products (WP) medium and i. wood products (WP) slow.

Second, there is a large shift in soil respiration loss under land-use change, with increasingly negative S2-S3 differences (Fig. 9b). In JULES, this reflects disturbance-driven acceleration of soil carbon turnover. It means a different fraction of biomass enters soil carbon pools as litter after conversion, altering the balance between soil-carbon inputs and heterotrophic losses. This finding aligns with other studies (Safitri et al., 2025, 2026). Harvest has almost no effect as the harvest setting is 25-year rotation (Fig. 9c). The wood products (WP) of dedicated oil palm PFT (Scenario 3) is consistently larger (more negative) than

https://doi.org/10.5194/egusphere-2026-3689
Preprint. Discussion started: 28 July 2026

WP of oil palm as generic cropland (Scenario 1), indicating greater transfer of biomass to product pools and their delayed released to atmosphere (Fig. 9g, 9h, 9i). Fire-related processes do not play a major role (Fig. 9d, 9e, 9f).

Over the early years of expansion, much conversion occurred on previously cleared land and rapid biomass accumulation in establishing plantations temporarily enhanced carbon uptake, partly offsetting net emissions. This is consistent with previous studies (Khasanah et al., 2015; Lewis et al., 2020; Meijide et al., 2020). However, from the late 2000s onwards, emissions increasingly reflect sustained soil carbon losses, enhanced heterotrophic respiration and transfer of forest biomass into shorter-lived product pools, consistent with previous observational and modelling evidence across Southeast Asian plantation landscapes (Comeau et al., 2016; Guillaume et al., 2018; Hergoualc'h et al., 2017; Safitri et al., 2024; Zhao et al., 2022).

3.4 Spatial patterns of ELUC

Spatial patterns of ELUC show that the impact of oil palm expansion varies across Indonesia (Fig. 10). To understand this, we separate the spatial signal into two components. Panel (a) shows the contribution of oil palm expansion to ELUC, calculated as the difference between simulations with (Scenario 3) and without (Scenario 2) oil palm. Panel (b) shows the bias introduced when oil palm is represented as a generic cropland (Scenario 1 minus Scenario 3).

Oil palm expansion is concentrated in specific regions (Fig. 10a). The largest increases in ELUC occur in Sumatra and Kalimantan, where oil palm plantations have expanded rapidly. The mean spatial ELUC is about 0.007 ± 0.032 kgC m^{-2} yr^{-1}, with a range from −0.114 to 0.309 kgC m^{-2} yr^{-1}. Oil palm expansion generally increases emissions relative to the non-palm scenario. Positive values dominate in areas undergoing recent conversion from natural vegetation into plantation, indicating increased ELUC associated with oil palm expansion. In contrast, regions with limited oil palm expansion show values close to zero, indicating that the effect is spatially constrained to areas of active land-use change.

The bias from mistreating oil palm as generic cropland seems to appear in the same regions of Sumatra and Kalimantan but to a lower magnitude (Fig. 10b). The mean bias ELUC is around 0.0015 ± 0.012 kgC m^{-2} yr^{-1}, with a range from −0.072 to 0.150 kgC m^{-2} yr^{-1}. Representing oil palm as generic cropland results in higher ELUC compared with using an explicit oil palm PFT, mainly in Sumatra and some parts of Kalimantan. This means that generic cropland does not fully capture the carbon dynamics of oil palm systems.

https://doi.org/10.5194/egusphere-2026-3689
Preprint. Discussion started: 28 July 2026

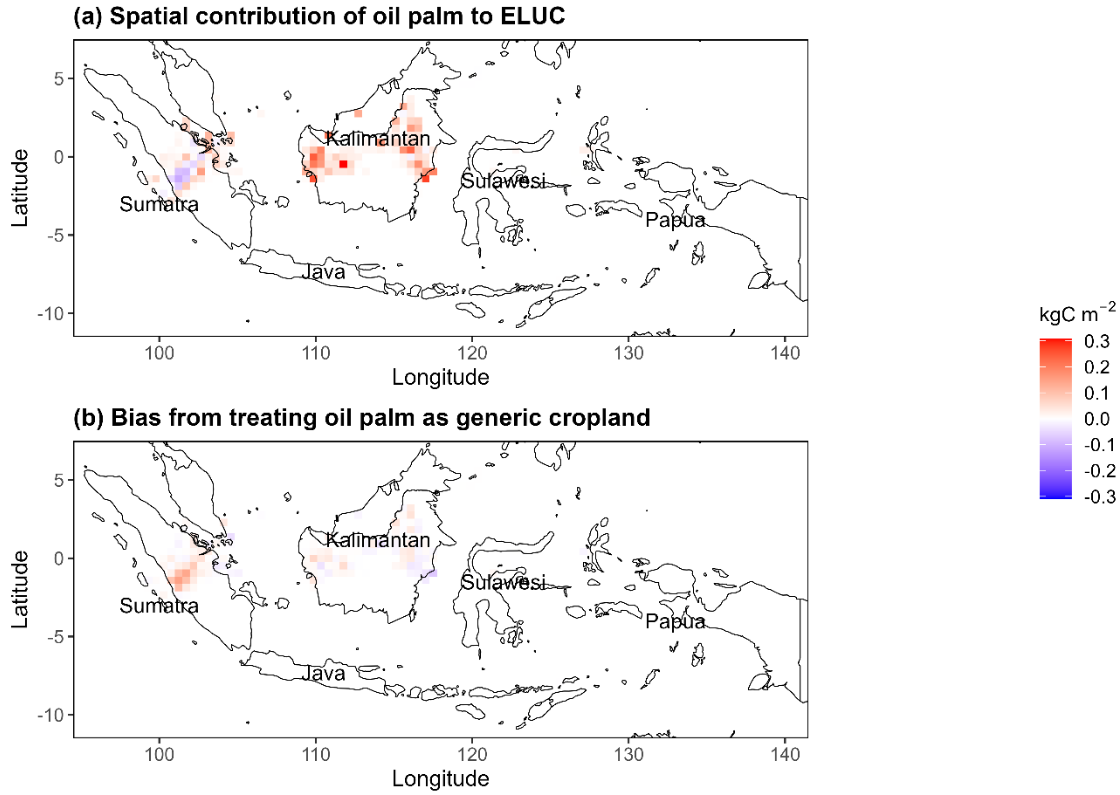

Figure 10: Spatial patterns of the effect of oil palm representation on cumulative land-use change carbon emissions (ELUC) in Indonesia over 2000–2022. (a) the contribution of oil palm expansion to ELUC, calculated as the difference between the explicit oil palm PFT simulation and the no-palm simulation and (b) the bias introduced when oil palm is represented as generic cropland, calculated as the difference between the generic-crop and explicit oil palm PFT simulations. Positive values indicate higher cumulative ELUC in the first scenario named in each panel.

Negative values in Figure 10a, particularly in parts of Sumatra, indicate locations where including oil palm results in lower ELUC than in the no-palm scenario. Analysis of carbon fluxes in these regions shows that this effect is driven by lower soil respiration losses under the oil palm PFT, mainly in the early stages of plantation. This lower soil respiration might reach up to ~0.2 kgC m^{-2} yr^{-1} during the peak period in these grid cells. Meanwhile, the productivity of the oil palm is consistently lower than the no-palm scenario. As a result, even though productivity is reduced, total carbon losses to the atmosphere are also reduced, producing a transient net decrease in ELUC. These negative values are spatially localised and reflect differences in modelled carbon cycling processes rather than a general reduction in emissions from oil palm expansion. Overall, this highlights the importance of soil carbon dynamics in determining the spatial variability of ELUC.

These spatial patterns are consistent with the national-scale results (Section 3.2) and the process-level analysis (Section 3.3). Regions with strong ELUC signals correspond to areas where changes in NPP and soil respiration are most pronounced

https://doi.org/10.5194/egusphere-2026-3689
Preprint. Discussion started: 28 July 2026

following land conversion. In particular, reduced productivity and enhanced soil carbon loss contribute to higher emissions in areas of recent plantation expansion. Overall, the results show that the impact of oil palm on ELUC depends not only on its total area but also on where expansion occurs. Accurately representing oil palm as a distinct PFT is therefore important for capturing both the magnitude and spatial distribution of land-use change emissions in Indonesia.

4 Discussion

This study focuses on developing a distinct oil palm PFT in JULES to better understand its role in the carbon cycle. It parameterises the model using available observations of oil palm structures and physiological characteristics. The model does not perfectly capture the oil palm plantation. Even after calibration, the model still has several limitations. It overestimates canopy height, while underestimating GPP for mature oil palm. However, the calibrated parameter settings represent a substantial improvement in characterising oil palm as a unique PFT. This development reduces the ambiguity in model outputs where oil palm is misclassified as a generic crop or a tropical evergreen tree (Harper et al., 2016).

The explicit oil palm PFT influenced the temporal dynamics/variation of annual ELUC, particularly in the period of rapid plantation. In several early years, the ELUC of the explicit oil palm PFT is lower than other scenarios. This reflects the rapid biomass accumulation in young oil palm compared with that in annual crops. However, this effect decreases over the long term, as the annual ELUC of explicit oil palm is close to the annual ELUC of oil palm as a generic crop after 15 years. This happens as biomass accumulation slows in mature plantations, while soil carbon losses increasingly offset NPP gains.

Large-scale oil palm expansion in Indonesia began around 1990, with approximately 7 million hectares (Mha) planted during that first decade (Carlson et al., 2012; FAO, 2022). Because the *Mapbiomas Indonesia* dataset used in this study begins in 2000, emissions associated with earlier plantation establishment are not explicitly represented. As a result, the simulation depicts a rapid increase in plantations at the start of the record. This may overestimate emissions in the early simulation years while underrepresenting legacy carbon fluxes from the previous decade.

There are further limitations in the current model configuration, e.g., it does not distinguish between peat and mineral soils. Peatlands are of particular significance in Southeast Asia, where a large proportion of oil palm plantations are established on peat soils (Miettinen et al., 2016; Page et al., 2011). The EC sites utilised in this study – Sabaju and Sebungan – are both located in peat swamp regions. The measurements show large peat carbon losses, with higher emissions at Sabaju than Sebungan. For example, reported heterotrophic respiration from peat was approximately 24 Mg CO_2-C ha^{-1} yr^{-1} at Sabaju and 11 Mg CO_2-C ha^{-1} yr^{-1} at Sebungan, while combined plantation peat carbon losses were estimated at about 96-97 Mg CO_2-eq ha^{-1} yr^{-1} at Sabaju and 48-51 Mg CO_2-eq ha^{-1} yr^{-1} at Sebungan (Manning et al., 2019). These values indicate that peat-related emissions can be of the same order of magnitude as, or even larger than, vegetation carbon-stock changes following land-use conversion. This means the observed fluxes include contributions from peat, which the model does not explicitly account for. This may result in an underestimation or misrepresentation of total carbon fluxes (Hirano et al., 2024; Wakhid et al., 2022;

https://doi.org/10.5194/egusphere-2026-3689
Preprint. Discussion started: 28 July 2026

Wakhid and Hirano, 2021). As more EC datasets become available in oil palm plantations, future research can refine this parameterisation.

The application of JULES-Palm should carefully consider harvest settings, based on research objectives. This study uses a periodic harvest formulation to approximate replanting plantations rather than routine fresh fruit bunch (FFB) harvesting. This configuration provides a clear signal of ecosystem carbon stock changes associated with land-use conversion, regrowth, and stand replacement, without conflating these effects with product export. However, it also means that regular FFB harvest is not explicitly represented in the current JULES-Palm configuration. This is an important limitation because FFB harvest removes reproductive carbon from the plantation as product, whereas the current model does not include a separate fruit carbon pool or a repeated fruit export pathway.

To assess the possible scale of this missing pathway, we calculated a first-order diagnostic of potential FFB-C export (Table 3). The low, mid and high estimates were based on a sensitivity range of 15, 20 and 30 t FFB ha^{-1} yr^{-1} (Siang et al., 2022; Teh and Sung, 2016; Zolfagharnassab et al., 2022). This range spans lower-yielding to high-yielding mature oil palm plantations and is consistent with reported FFB productivity values from Indonesian plantations and wider oil palm literature. Fresh FFB yield was converted to carbon using a dry matter fraction of 0.50 and a carbon fraction of 0.577 (Wakhid et al., 2022; Wakhid and Hirano, 2021). Based on these assumptions, mature FFB-C export was estimated as 4.33-8.65 tC ha^{-1} yr^{-1}, with a mid-estimate of 5.77 tC ha^{-1} yr^{-1}. This corresponds to approximately 34-35 % of annual oil palm NPP. Applying an age-yield ramp to oil palm area added after 2000 gives an expansion-related gross FFB-C export estimate of 0.334-0.668 PgC over 2000-2022.

Table 3 First-order scale diagnostic for potential missing fresh fruit bunch carbon export. Mature FFB-C export was estimated using literature-based assumptions for fresh fruit bunch yield, dry matter fraction and carbon content.

Diagnostic	Low	Mid	High	Interpretation	Main_source_or_basis
Mature FFB-C export	4.33 tC ha^{-1} yr^{-1}	5.77 tC ha^{-1} yr^{-1}	8.65 tC ha^{-1} yr^{-1}	Gross product carbon potentially exported from mature oil palm plantations.	FFB yield sensitivity range; dry matter fraction = 0.50 and C fraction = 0.577 from (Wakhid and Hirano, 2021).
FFB-C export / annual NPP	34.0 %	34.5 %	35.0 %	Approximate share of annual oil palm productivity allocated to fruit bunches.	Fruit bunch production share of NPP from (Wakhid et al., 2022).

https://doi.org/10.5194/egusphere-2026-3689
Preprint. Discussion started: 28 July 2026

Expansion-related gross FFB-C export, 2000–2022	0.334 PgC	0.445 PgC	0.668 PgC	Gross product export associated with post-2000 expansion; not applied as a direct ELUC correction.	Calculated from MapBiomas oil palm expansion, age-yield ramp, and FFB-C export assumptions.

These values should not be interpreted as a direct correction to simulated ELUC, because FFB harvest is a gross product-export flux, whereas ELUC is a net land-use-change carbon-balance term. In the current model, the fate of carbon that would otherwise be exported as FFB depends on vegetation turnover, litter decomposition and soil respiration, and cannot be isolated without explicitly tracking a fruit carbon pool. The diagnostic therefore indicates that FFB harvest is a substantial missing carbon pathway, but it is not applied as a formal correction to ELUC. Future development of JULES-Palm should prioritise an explicit reproductive carbon pool and repeated FFB harvest export, similar to recent oil palm implementations in other land-surface models (Xu et al., 2021).

In the wider context of the global land surface, the question of how best to represent oil palm remains critical. Given its rapid expansion over recent decades, the contribution of oil palm to carbon emissions, land surface albedo and energy balance cannot be neglected (Brasika et al., 2025; Xu et al., 2021), especially when it is converted from peat-swamp forests. Establishing a dedicated oil palm PFT provides the most robust and scientifically defensible means of representing its unique physiological and ecological properties. Nevertheless, in the absence of a specialised PFT, representing oil palm under a generalised “crop” or “agriculture” category remains a reasonable interim solution to capture first-order land-use change carbon emissions.

5 Conclusion

This research shows the first implementation of oil palm (*Elaeis guineensis*) as an explicit PFT within JULES. The parameters adjust the key characteristics of oil palm, including the photosynthesis process (GPP), structural allometry (LAI, AGB, and canopy height), and oil palm management (plantation and harvest). There are significant improvements in the oil palm PFT after evaluation and calibration with available EC flux measurements and field allometry measurements. It accurately captures photosynthesis in young oil palm and reduces overestimations of AGB and canopy height.

The JULES-Palm plays a key role in improving our understanding of the contribution of oil palm in land-use change emissions in Indonesia. The explicit oil palm representation increases mean annual ELUC from 0.052 ± 0.010 to 0.058 ± 0.012 PgC yr^{-1} for the period of 2000-2022. Meanwhile, representing oil palm as generic cropland overestimates the magnitude of emissions (0.066 ± 0.011 PgC yr^{-1}). Cumulative emissions of ~0.14 PgC are attributed to oil palm expansion, accounting for about 10.3% of Indonesia’s total ELUC when legacy fluxes are included, and approximately 89% of land-use change fluxes attributable to conversion occurring during the study period. Thus, an explicit oil palm PFT reduces bias by capturing rapid early-stage biomass accumulation, delayed respiration and soil carbon responses. In addition, the spatial analysis shows that this impact is highly heterogeneous, with emission hotspots concentrated in Sumatra and Kalimantan where extensive land conversion occurs. These results demonstrate that oil palm expansion has a measurable, regionally significant impact on Indonesia's land carbon balance.

Overall, JULES-Palm represents an important improvement in modelling tropical plantations, enabling a more robust carbon budget assessment with realistic process attribution. However, the extent and timing of land use conversion remain critical drivers of ELUC. As oil palm expands in tropical landscapes, further development, including completing pre-2000 land-use history, peat-specific processes, and better harvest representation, might increase accuracy.

6 Code Availability

The JULES code used in these simulations is available from the Met Office's Science Repository Service with suite u-ea492 at https://code.metoffice.gov.uk/trac/roses-u/browser/e/a/4/9/2/trunk/app/jules/rose-app.conf?rev=359798.

7 Data Availability

The JULES-Palm output can be accessed at https://doi.org/10.5281/zenodo.21070341 (Brasika, 2026). Legacy flux is available at https://doi.org/10.5281/zenodo.15552386 (Brasika, 2025). The Mapbiomas data are freely available at https://mapbiomas.nusantara.earth, last access: 11 December 2025 (Mapbiomas Indonesia, 2022). The observation datasets of EC and allometric can be accessed through its associated publications (detailed in Supplement).

8 Supplement

9 Author Contribution

IBMB, PF, SS & MOS designed the ideas and methodology. MCDR set up JULES running for hypercube sampling. EL & IBMB developed the JULES-Palm initial configuration. TM & IBMB evaluated parameters of oil palm in JULES. TH prepared eddy covariance dataset. AK, TJ & LS evaluated the dataset. WL, MK, YF, XL, RZ, YX, & JZ benchmarked the model development with other models. YF, YX, provide allometric datasets. DS & TM prepare the oil palm land use dataset. IBMB and PF led the writing of the manuscript to which all authors contributed.

9 Competing interests

The contact author has declared that none of the authors has any competing interests.

10 Acknowledgements

Ida Bagus Mandhara Brasika thanks Indonesian Endowment Fund, also known as LPDP (Lembaga Pengelola Dana Pendidikan) for the PhD scholarship. This study was supported by the University of Exeter through central OA funds and Tsinghua University Initiative Scientific Research Program. Masayuki Kondo and Ida Bagus Mandhara Brasika acknowledge support from the League of Geophysical Research eXcellences for Tropical Asia (LeXtra), which is endorsed by the Integrated Land Ecosystem-Atmosphere Processes Study (iLEAPS) and the Global Carbon Project (GCP) Tsukuba International Office. Maria Carolina Duran-Rojas has received funding from the European Research Council (ERC) under the European Union's Horizon 2020 research and innovation programme (grant agreement No 865403). Emma W. Littleton acknowledges support from the European Commission's Horizon 2020 research and innovation programme under grant agreements 101060554 (OptFor-EU) and 101003536 (ESM2025), and from UKRI-BBSRC award BB/V011588/1 (NetZeroPlus). Alexander Knohl and Tejaswini Jaajpera acknowledge funding from the German Research Foundation (ClimReg project number 532868192 and German-Indonesian Research Collaborative Research Center 990: Ecological and Socioeconomic Functions of Tropical Lowland Rainforest Transformation Systems (EFForTS) project number 192626868)

References

Agus, F., Gunarso, P., Sahardjo, B. H., Harris, N., Van Noordwijk, M., and Killeen, T. J.: Historical CO2 emissions from land use and land use change from the oil palm industry in Indonesia, Malaysia and Papua New Guinea, 2013.

Ali, A. A., Nugroho, B., Moyano, F. E., Brambach, F., Jenkins, M. W., Pangle, R., Stiegler, C., Blei, E., Cahyo, A. N., Olchev, A., Irawan, B., Ariani, R., June, T., Tarigan, S., Corre, M. D., Veldkamp, E., and Knohl, A.: Using a bottom-up approach to scale leaf photosynthetic traits of oil palm, rubber, and two coexisting tropical woody species, Forests, 12, https://doi.org/10.3390/f12030359, 2021.

Austin, K. G., Schwantes, A., Gu, Y., and Kasibhatla, P. S.: What causes deforestation in Indonesia?, Environmental Research Letters, 14, https://doi.org/10.1088/1748-9326/aaf6db, 2019.

Awal, M. A., Ishak, W. I. W., and Bockari-Gevao, S. M.: Determination of Leaf Area Index for Oil Palm Plantation Using Hemispherical Photography Technique, Pertanika J. Sci. & Technol, 23–32 pp., 2010.

Bayona-Rodriguez, C. J. and Romero, H. M.: Physiological and agronomic behavior of commercial cultivars of oil palm (Elaeis guineensis) and OxG hybrids (Elaeis oleifera x Elaeis guineensis) at rainy and dry seasons, Aust. J. Crop Sci., 13, 424–432, https://doi.org/10.21475/ajcs.19.13.03.p1354, 2019.

Best, M. J., Pryor, M., Clark, D. B., Rooney, G. G., Essery, R. . L. H., Ménard, C. B., Edwards, J. M., Hendry, M. A., Porson, A., Gedney, N., Mercado, L. M., Sitch, S., Blyth, E., Boucher, O., Cox, P. M., Grimmond, C. S. B., and Harding, R. J.: The Joint UK Land Environment Simulator (JULES), model description – Part 1: Energy and water fluxes, Geosci. Model Dev., 4, 677–699, https://doi.org/10.5194/gmd-4-677-2011, 2011.

Bloom, A. A. and Williams, M.: Constraining ecosystem carbon dynamics in a data-limited world: Integrating ecological "common sense" in a model-data fusion framework, Biogeosciences, 12, 1299–1315, https://doi.org/10.5194/bg-12-1299-2015, 2015.

Brasika, I. B. M.: JULES-ES of carbon emissions from land use change (ELUC) in Indonesia, https://doi.org/10.5281/zenodo.15552386, 2025.

Brasika, I. B. M.: JULES-Palm of carbon emissions from land use change (ELUC) in Indonesia with explicit oil palm, https://doi.org/10.5281/zenodo.21070341, 30 June 2026.

Brasika, I. B. M., Friedlingstein, P., Sitch, S., O'Sullivan, M., Duran-Rojas, M. C., Rosan, T. M., Goldewijk, K. K., Pongratz, J., Schwingshackl, C., Chini, L. P., and Hurtt, G. C.: Uncertainties in carbon emissions from land use and land cover change in Indonesia, Biogeosciences, 22, 3547–3561, https://doi.org/10.5194/bg-22-3547-2025, 2025.

Breure, C. J.: Factors influencing the variation in canopy light extinction coefficient (k) among pisifera parents of two oil palm origins, Exp. Agric., 60, https://doi.org/10.1017/S0014479724000073, 2024.

Burton, C., Betts, R., Cardoso, M., Feldpausch, R. T., Harper, A., Jones, C. D., Kelley, D. I., Robertson, E., and Wiltshire, A.: Representation of fire, land-use change and vegetation dynamics in the Joint UK Land Environment Simulator vn4.9 (JULES), Geosci. Model Dev., 12, 179–193, https://doi.org/10.5194/gmd-12-179-2019, 2019.

Carlson, K. M., Curran, L. M., Ratnasari, D., Pittman, A. M., Soares-Filho, B. S., Asner, G. P., Trigg, S. N., Gaveau, D. A., Lawrence, D., and Rodrigues, H. O.: Committed carbon emissions, deforestation, and community land conversion from oil palm plantation expansion in West Kalimantan, Indonesia, Proc. Natl. Acad. Sci. U. S. A., 109, 7559–7564, https://doi.org/10.1073/pnas.1200452109, 2012.

Cheah, S. S. and Teh, C. B. S.: Parameterization of the farquhar-von caemmerer-berry c3 photosynthesis model for oil palm, Photosynthetica, 58, 769–779, https://doi.org/10.32615/ps.2020.020, 2020.

Clark, D. B., Mercado, L. M., Sitch, S., Jones, C. D., Gedney, N., Best, M. J., Pryor, M., Rooney, G. G., Essery, R. L. H., Blyth, E., Boucher, O., Harding, R. J., Huntingford, C., and Cox, P. M.: The Joint UK Land Environment Simulator (JULES), model description – Part 2: Carbon fluxes and vegetation dynamics, Geosci. Model Dev., 4, 701–722, https://doi.org/10.5194/gmd-4-701-2011, 2011.

Clough, Y., Krishna, V. V., Corre, M. D., Darras, K., Denmead, L. H., Meijide, A., Moser, S., Musshoff, O., Steinebach, S., Veldkamp, E., Allen, K., Barnes, A. D., Breidenbach, N., Brose, U., Buchori, D., Daniel, R., Finkeldey, R., Harahap, I., Hertel, D., Holtkamp, A. M., Hörandl, E., Irawan, B., Jaya, I. N. S., Jochum, M., Klarner, B., Knohl, A., Kotowska, M. M., Krashevska, V., Kreft, H., Kurniawan, S., Leuschner, C., Maraun, M., Melati, D. N., Opfermann, N., Pérez-Cruzado, C., Prabowo, W. E., Rembold, K., Rizali, A., Rubiana, R., Schneider, D., Tjitrosoedirdjo, S. S., Tjoa, A., Tscharntke, T., and Scheu, S.: Land-use choices follow profitability at the expense of ecological functions in Indonesian smallholder landscapes, Nat. Commun., 7, https://doi.org/10.1038/ncomms13137, 2016.

https://doi.org/10.5194/egusphere-2026-3689
Preprint. Discussion started: 28 July 2026

Comeau, L. P., Hergoualc'h, K., Hartill, J., Smith, J., Verchot, L. V., Peak, D., and Salim, A. M.: How do the heterotrophic and the total soil respiration of an oil palm plantation on peat respond to nitrogen fertilizer application?, Geoderma, 268, 41–51, https://doi.org/10.1016/j.geoderma.2016.01.016, 2016.

Cook, S., Whelan, M. J., Evans, C. D., Gauci, V., Peacock, M., Garnett, M. H., Kho, L. K., Teh, Y. A., and Page, S. E.: Fluvial organic carbon fluxes from oil palm plantations on tropical peatland, Biogeosciences, 15, 7435–7450, https://doi.org/10.5194/bg-15-7435-2018, 2018.

Cooper, H. V., Evers, S., Aplin, P., Crout, N., Dahalan, M. P. Bin, and Sjogersten, S.: Greenhouse gas emissions resulting from conversion of peat swamp forest to oil palm plantation, Nat. Commun., 11, https://doi.org/10.1038/s41467-020-14298-w, 2020.

Corley, R. H. V. . and Tinker, P. B. .: The oil palm, John Wiley & Sons, 2016.

Cox, P. M.: Description of the "TRIFFID" Dynamic Global Vegetation Model, 2001.

Danylo, O., Pirker, J., Lemoine, G., Ceccherini, G., See, L., McCallum, I., Hadi, Kraxner, F., Achard, F., and Fritz, S.: A map of the extent and year of detection of oil palm plantations in Indonesia, Malaysia and Thailand, Sci. Data, 8, https://doi.org/10.1038/s41597-021-00867-1, 2021.

Dermoredjo, S. K., Darmawan, D. H. A., Sumedi, Mutaqin, Dani, F. Z. D. P., Yusuf, E. S., Pasaribu, S. M., Sayaka, B., Wardana, I. P., Adnyana, I. M. O., Estiningtyas, W., and Antriyandarti, E.: The global sway of Indonesian palm oil: An export analysis, J. Agric. Food Res., 22, https://doi.org/10.1016/j.jafr.2025.102064, 2025.

Dufrene, E. and Saugier, B.: Gas Exchange of Oil Palm in Relation to Light, Vapour Pressure Deficit, Temperature and Leaf Age, Ecology, 97–104 pp., 1993.

Fan, Y., Roupsard, O., Bernoux, M., Le Maire, G., Panferov, O., Kotowska, M. M., and Knohl, A.: A sub-canopy structure for simulating oil palm in the Community Land Model (CLM-Palm): Phenology, allocation and yield, Geosci. Model Dev., 8, 3785–3800, https://doi.org/10.5194/gmd-8-3785-2015, 2015.

Fan, Y., Meijide, A., Lawrence, D. M., Roupsard, O., Carlson, K. M., Chen, H. Y., Röll, A., Niu, F., and Knohl, A.: Reconciling Canopy Interception Parameterization and Rainfall Forcing Frequency in the Community Land Model for Simulating Evapotranspiration of Rainforests and Oil Palm Plantations in Indonesia, J. Adv. Model. Earth Syst., 11, 732–751, https://doi.org/10.1029/2018MS001490, 2019.

FAO: FAOSTAT Land Use database - Country Note, 2022.

Friedlingstein, P., O'Sullivan, M., Jones, M. W., Andrew, R. M., Bakker, D. C. E., Hauck, J., Landschützer, P., Le Quéré, C., Luijkx, I. T., Peters, G. P., Peters, W., Pongratz, J., Schwingshackl, C., Sitch, S., Canadell, J. G., Ciais, P., Jackson, R. B., Alin, S. R., Anthoni, P., Barbero, L., Bates, N. R., Becker, M., Bellouin, N., Decharme, B., Bopp, L., Brasika, I. B. M., Cadule, P., Chamberlain, M. A., Chandra, N., Chau, T.-T.-T., Chevallier, F., Chini, L. P., Cronin, M., Dou, X., Enyo, K., Evans, W., Falk, S., Feely, R. A., Feng, L., Ford, D. J., Gasser, T., Ghattas, J., Gkritzalis, T., Grassi, G., Gregor, L., Gruber, N., Gürses, Ö., Harris, I., Hefner, M., Heinke, J., Houghton, R. A., Hurtt, G. C., Iida, Y., Ilyina, T., Jacobson, A. R., Jain, A., Jarníková, T., Jersild, A., Jiang, F., Jin, Z., Joos, F., Kato, E., Keeling, R. F., Kennedy, D., Klein Goldewijk, K., Knauer, J., Korsbakken,

https://doi.org/10.5194/egusphere-2026-3689
Preprint. Discussion started: 28 July 2026

J. I., Körtzinger, A., Lan, X., Lefèvre, N., Li, H., Liu, J., Liu, Z., Ma, L., Marland, G., Mayot, N., McGuire, P. C., McKinley, G. A., Meyer, G., Morgan, E. J., Munro, D. R., Nakaoka, S.-I., Niwa, Y., O'Brien, K. M., Olsen, A., Omar, A. M., Ono, T., Paulsen, M., Pierrot, D., Pocock, K., Poulter, B., Powis, C. M., Rehder, G., Resplandy, L., Robertson, E., Rödenbeck, C., Rosan, T. M., Schwinger, J., Séférian, R., et al.: Global Carbon Budget 2023, Earth Syst. Sci. Data, 15, 5301–5369, https://doi.org/10.5194/essd-15-5301-2023, 2023.

Friedlingstein, P., O'Sullivan, M., Jones, M. W., Andrew, R. M., Bakker, D. C. E., Hauck, J., Landschützer, P., Le Quéré, C., Li, H., Luijkx, I. T., Peters, G. P., Peters, W., Pongratz, J., Schwingshackl, C., Sitch, S., Canadell, J. G., Ciais, P., Aas, K., Alin, S. R., Anthoni, P., Barbero, L., Bates, N. R., Bellouin, N., Benoit-Cattin, A., Berghoff, C. F., Bernardello, R., Bopp, L., Brasika, I. B. M., Chamberlain, M. A., Chandra, N., Chevallier, F., Chini, L. P., Collier, N. O., Colligan, T. H., Cronin, M., Djeutchouang, L. M., Dou, X., Enright, M. P., Enyo, K., Erb, M., Evans, W., Feely, R. A., Feng, L., Ford, D. J., Foster, A., Fransner, F., Gasser, T., Gehlen, M., Gkritzalis, T., Goncalves De Souza, J., Grassi, G., Gregor, L., Gruber, N., Guenet, B., Gürses, Ö., Harrington, K., Harris, I., Heinke, J., Hurtt, G. C., Iida, Y., Ilyina, T., Ito, A., Jacobson, A. R., Jain, A. K., Jarníková, T., Jersild, A., Jiang, F., Jones, S. D., Kato, E., Keeling, R. F., Klein Goldewijk, K., Knauer, J., Kong, Y., Korsbakken, J. I., Koven, C., Kunimitsu, T., Lan, X., Liu, J., Liu, Z., Liu, Z., Lo Monaco, C., Ma, L., Marland, G., McGuire, P. C., McKinley, G. A., Melton, J. R., Monacci, N., Monier, E., Morgan, E. J., Munro, D. R., Müller, J. D., Nakaoka, S.-I., Nayagam, L. R., Niwa, Y., Nutzel, T., Olsen, A., Omar, A. M., Pan, N., Pandey, S., et al.: Global Carbon Budget 2025, Earth Syst. Sci. Data, 18, 3211–3288, https://doi.org/10.5194/essd-18-3211-2026, 2026.

Gaveau, D. L. A., Locatelli, B., Salim, M. A., Husnayaen, Manurung, T., Descals, A., Angelsen, A., Meijaard, E., and Sheil, D.: Slowing deforestation in Indonesia follows declining oil palm expansion and lower oil prices, PLoS One, 17, https://doi.org/10.1371/journal.pone.0266178, 2022.

Guillaume, T., Kotowska, M. M., Hertel, D., Knohl, A., Krashevska, V., Murtilaksono, K., Scheu, S., and Kuzyakov, Y.: Carbon costs and benefits of Indonesian rainforest conversion to plantations, Nat. Commun., 9, https://doi.org/10.1038/s41467-018-04755-y, 2018.

Harper, A., Cox, P. M., Friedlingstein, P., Wiltshire, A. J., Jones, C. D., Sitch, S., Mercado, L. M., Groenendijk, M., Robertson, E., Kattge, J., Bönisch, G., Atkin, O. K., Bahn, M., Cornelissen, J., Niinemets, Ü., Onipchenko, V., Peñuelas, J., Poorter, L., Reich, P. B., Soudzilovskaia, N. A., and Bodegom, P. van: Improved representation of plant functional types and physiology in the Joint UK Land Environment Simulator (JULES v4.2) using plant trait information, Geosci. Model Dev., 9, 2415–2440, https://doi.org/10.5194/gmd-9-2415-2016, 2016.

Harper, A. B., Wiltshire, A. J., Cox, P. M., Friedlingstein, P., Jones, C. D., Mercado, L. M., Sitch, S., Williams, K., and Duran-Rojas, C.: Vegetation distribution and terrestrial carbon cycle in a carbon cycle configuration of JULES4.6 with new plant functional types, Geosci. Model Dev., 11, 2857–2873, https://doi.org/10.5194/gmd-11-2857-2018, 2018.

Harris, N. L., Gibbs, D. A., Baccini, A., Birdsey, R. A., de Bruin, S., Farina, M., Fatoyinbo, L., Hansen, M. C., Herold, M., Houghton, R. A., Potapov, P. V., Suarez, D. R., Roman-Cuesta, R. M., Saatchi, S. S., Slay, C. M., Turubanova, S. A., and

https://doi.org/10.5194/egusphere-2026-3689
Preprint. Discussion started: 28 July 2026

Tyukavina, A.: Global maps of twenty-first century forest carbon fluxes, Nat. Clim. Chang., 11, 234–240, https://doi.org/10.1038/s41558-020-00976-6, 2021.

Hergoualc'h, K., Hendry, D. T., Murdiyarso, D., and Verchot, L. V.: Total and heterotrophic soil respiration in a swamp forest and oil palm plantations on peat in Central Kalimantan, Indonesia, Biogeochemistry, 135, 203–220, https://doi.org/10.1007/s10533-017-0363-4, 2017.

Hirano, T., Ohkubo, S., Itoh, M., Tsuzuki, H., Sakabe, A., Takahashi, H., Kusin, K., and Osaki, M.: Large variation in carbon dioxide emissions from tropical peat swamp forests due to disturbances, Commun. Earth Environ., 5, https://doi.org/10.1038/s43247-024-01387-7, 2024.

Ida Sunaryathy, P., Devi Kanniah, K., and Pang Tan, K.: Estimating Aboveground Biomass of Oil Palm Trees by Using the Destructive Method, World J. Agric. Res., 3, 17–19, https://doi.org/10.12691/wjar-3-1-4, 2015.

Intara, Y. I., Nusantara, A. D., Supanjani, Caniago, Z., and Ekawita, R.: Oil Palm Roots Architecture in Response to Soil Humidity, International Journal of Oil Palm, 1, 79–89, 2018.

Khasanah, N., van Noordwijk, M., and Ningsih, H.: Aboveground carbon stocks in oil palm plantations and the threshold for carbon-neutral vegetation conversion on mineral soils, Cogent Environ. Sci., 1, https://doi.org/10.1080/23311843.2015.1119964, 2015.

Koh, L. P., Zeng, Y., Sarira, T. V., and Siman, K.: Carbon prospecting in tropical forests for climate change mitigation, Nat. Commun., 12, https://doi.org/10.1038/s41467-021-21560-2, 2021.

Kotowska, M. M., Leuschner, C., Triadiati, T., Meriem, S., and Hertel, D.: Quantifying above- and belowground biomass carbon loss with forest conversion in tropical lowlands of Sumatra (Indonesia), Glob. Chang. Biol., 21, 3620–3634, https://doi.org/10.1111/gcb.12979, 2015.

Kulpanich, N., Worachairungreung, M., Waiyasusri, K., Sae-Ngow, P., and Pinasu, D.: Height measurement and oil palm yield prediction using Unmanned Aerial Vehicle (UAV) data to create Canopy Height Model (CHM), Geographia Technica, 17, 164–178, https://doi.org/10.21163/GT_2022.172.14, 2022.

Lewis, K., Rumpang, E., Kho, L. K., McCalmont, J., Teh, Y. A., Gallego-Sala, A., and Hill, T. C.: An assessment of oil palm plantation aboveground biomass stocks on tropical peat using destructive and non-destructive methods, Sci. Rep., 10, https://doi.org/10.1038/s41598-020-58982-9, 2020.

Lim, F. K. S., Carrasco, L. R., Edwards, D. P., and McHardy, J.: Land-use change from market responses to oil palm intensification in Indonesia, Conservation Biology, 38, https://doi.org/10.1111/cobi.14149, 2024.

Littleton, E. W., Harper, A. B., Vaughan, N. E., Oliver, R. J., Duran-Rojas, M. C., and Lenton, T. M.: JULES-BE: Representation of bioenergy crops and harvesting in the Joint UK Land Environment Simulator vn5.1, Geosci. Model Dev., 13, 1123–1136, https://doi.org/10.5194/gmd-13-1123-2020, 2020.

Manning, F. C., Kho, L. K., Hill, T. C., Cornulier, T., and Teh, Y. A.: Carbon Emissions From Oil Palm Plantations on Peat Soil, Frontiers in Forests and Global Change, 2, https://doi.org/10.3389/ffgc.2019.00037, 2019.

Experts from the Asian country were trained by the Brazilian MapBiomas team to launch the land use mapping platform:

https://doi.org/10.5194/egusphere-2026-3689
Preprint. Discussion started: 28 July 2026

Mapbiomas Indonesia: https://mapbiomas.nusantara.earth/, last access: 11 December 2022.

McCalmont, J., Kho, L. K., Teh, Y. A., Lewis, K., Chocholek, M., Rumpang, E., and Hill, T.: Short- and long-term carbon emissions from oil palm plantations converted from logged tropical peat swamp forest, Glob. Chang. Biol., 27, 2361–2376, https://doi.org/10.1111/gcb.15544, 2021.

Meijide, A., de la Rua, C., Guillaume, T., Röll, A., Hassler, E., Stiegler, C., Tjoa, A., June, T., Corre, M. D., Veldkamp, E., and Knohl, A.: Measured greenhouse gas budgets challenge emission savings from palm-oil biodiesel, Nat. Commun., 11, https://doi.org/10.1038/s41467-020-14852-6, 2020.

Miettinen, J., Shi, C., and Liew, S. C.: Land cover distribution in the peatlands of Peninsular Malaysia, Sumatra and Borneo in 2015 with changes since 1990, Glob. Ecol. Conserv., 6, 67–78, https://doi.org/10.1016/j.gecco.2016.02.004, 2016.

Murphy, D. J., Goggin, K., and Paterson, R. R. M.: Oil palm in the 2020s and beyond: challenges and solutions, CABI Agriculture and Bioscience, 2, https://doi.org/10.1186/s43170-021-00058-3, 2021.

Nelson, P. N., Banabas, M., Scotter, D. R., and Webb, M. J.: Using soil water depletion to measure spatial distribution of root activity in oil palm (Elaeis guineensis Jacq.) plantations, Plant Soil, 286, 109–121, https://doi.org/10.1007/s11104-006-9030-6, 2006.

Van Oijen, M., Rougier, J., and Smith, R.: Bayesian calibration of process-based forest models: bridging the gap between models and data, Tree Physiol., 25, 915–927, 2005.

Oliver, R. J., Mercado, L. M., Clark, D. B., Huntingford, C., Taylor, C. M., Vidale, P. L., McGuire, P. C., Todt, M., Folwell, S., Shamsudheen Semeena, V., and Medlyn, B. E.: Improved representation of plant physiology in the JULES-vn5.6 land surface model: Photosynthesis, stomatal conductance and thermal acclimation, https://doi.org/10.5194/gmd-2022-11, 14 March 2022.

Page, S. E., Rieley, J. O., and Banks, C. J.: Global and regional importance of the tropical peatland carbon pool, Glob. Chang. Biol., 17, 798–818, https://doi.org/10.1111/j.1365-2486.2010.02279.x, 2011.

Perez, R. P. A., Vezy, R., Brancheriau, L., Boudon, F., Grand, F., Ramel, M., Doni, A., Raharjo, J.-P., and Caliman, J.: When architectural plasticity fails to counter the light competition imposed by planting design: an in silico approach using a functional-structural model of oil palm, https://doi.org/10.1093/insilicoplants/diac009, 2022.

Qaim, M., Sibhatu, K. T., Siregar, H., and Grass, I.: Environmental, Economic, and Social Consequences of the Oil Palm Boom, Annu. Rev. Resour. Economics, 12, 321–344, https://doi.org/10.1146/annurev-resource-110119, 2025.

Ramdani, F. and Hino, M.: Land Use Changes and GHG Emissions from Tropical Forest Conversion by Oil Palm Plantations in Riau Province, Indonesia, PLoS One, 8, https://doi.org/10.1371/journal.pone.0070323, 2013.

Rey-Sánchez, A. C., Slot, M., Posada, J. M., and Kitajima, K.: Spatial and seasonal variation in leaf temperature within the canopy of a tropical forest, Clim. Res., 71, 75–89, https://doi.org/10.3354/cr01427, 2016.

Rittgers, C., Mcdonald, G., and Rahmanulloh, A.: Indonesia Oilseeds and Products Annual Indonesia Oilseeds and Products Annual 2019, 2019.

Röll, A., Niu, F., Meijide, A., Ahongshangbam, J., Ehbrecht, M., Guillaume, T., Gunawan, D., Hardanto, A., Hendrayanto, Hertel, D., Kotowska, M. M., Kreft, H., Kuzyakov, Y., Leuschner, C., Nomura, M., Polle, A., Rembold, K., Sahner, J., Seidel, D., Zemp, D. C., Knohl, A., and Hölscher, D.: Transpiration on the rebound in lowland Sumatra, Agric. For. Meteorol., 274, 160–171, https://doi.org/10.1016/j.agrformet.2019.04.017, 2019.

Sabajo, C. R., Le Maire, G., June, T., Meijide, A., Roupsard, O., and Knohl, A.: Expansion of oil palm and other cash crops causes an increase of the land surface temperature in the Jambi province in Indonesia, Biogeosciences, 14, 4619–4635, https://doi.org/10.5194/bg-14-4619-2017, 2017.

Safitri, L., Galdos, M. V., Comber, A., and Challinor, A.: Potential for low-emissions oil palm production in Indonesia: insights from spatiotemporal dynamics, Environmental Research Letters, 19, https://doi.org/10.1088/1748-9326/ad404a, 2024.

Safitri, L., Galdos, M. V, Pradiko, I., Comber, A., and Challinor, A.: Characterising Climate Mitigation and Adaptation Performance through Spatiotemporal Productivity and Carbon Balance in Oil Palm Production, SSRN (preprint), https://doi.org/doi.org/10.2139/ssrn.5217519, 2025.

Safitri, L., Galdos, M. V., Pradiko, I., Comber, A., and Challinor, A.: Assessing climate-smartness of agronomic practices in oil palm production under changing climate conditions, European Journal of Agronomy, 174, https://doi.org/10.1016/j.eja.2025.127966, 2026.

Salvucci, M. E. and Crafts-Brandner, S. J.: Relationship between the heat tolerance of photosynthesis and the thermal stability of rubisco activase in plants from contrasting thermal environments, Plant Physiol., 134, 1460–1470, https://doi.org/10.1104/pp.103.038323, 2004.

Shigetomi, Y., Ishimura, Y., and Yamamoto, Y.: Trends in global dependency on the Indonesian palm oil and resultant environmental impacts, Sci. Rep., 10, https://doi.org/10.1038/s41598-020-77458-4, 2020.

Siang, C. S., Wahid, S. A. A., and Sung, C. T. B.: Standing Biomass, Dry-Matter Production, and Nutrient Demand of Tenera Oil Palm, Agronomy, 12, https://doi.org/10.3390/agronomy12020426, 2022.

Sitch, S., Friedlingstein, P., Gruber, N., Jones, S. D., Murray-Tortarolo, G., Ahlström, A., Doney, S. C., Graven, H., Heinze, C., Huntingford, C., Levis, S., Levy, P. E., Lomas, M., Poulter, B., Viovy, N., Zaehle, S., Zeng, N., Arneth, A., Bonan, G., Bopp, L., Canadell, J. G., Chevallier, F., Ciais, P., Ellis, R., Gloor, M., Peylin, P., Piao, S. L., Le Quéré, C., Smith, B., Zhu, Z., and Myneni, R.: Recent trends and drivers of regional sources and sinks of carbon dioxide, Biogeosciences, 12, 653–679, https://doi.org/10.5194/bg-12-653-2015, 2015.

Sitch, S., O'Sullivan, M., Robertson, E., Friedlingstein, P., Albergel, C., Anthoni, P., Arneth, A., Arora, V. K., Bastos, A., Bastrikov, V., Bellouin, N., Canadell, J. G., Chini, L., Ciais, P., Falk, S., Harris, I., Hurtt, G., Ito, A., Jain, A. K., Jones, M. W., Joos, F., Kato, E., Kennedy, D., Klein Goldewijk, K., Kluzek, E., Knauer, J., Lawrence, P. J., Lombardozzi, D., Melton, J. R., Nabel, J. E. M. S., Pan, N., Peylin, P., Pongratz, J., Poulter, B., Rosan, T. M., Sun, Q., Tian, H., Walker, A. P., Weber, U., Yuan, W., Yue, X., and Zaehle, S.: Trends and Drivers of Terrestrial Sources and Sinks of Carbon Dioxide: An Overview of the TRENDY Project, Global Biogeochem. Cycles, 38, https://doi.org/10.1029/2024GB008102, 2024.

https://doi.org/10.5194/egusphere-2026-3689
Preprint. Discussion started: 28 July 2026

Tan, K. P., Kanniah, K. D., and Cracknell, A. P.: On the upstream inputs into the MODIS primary productivity products using biometric data from oil palm plantations, Int. J. Remote Sens., 35, 2215–2246, https://doi.org/10.1080/01431161.2014.889865, 2014.

Teh, C. and Sung, B.: Availability, use, and removal of oil palm biomass in Indonesia, 2016.

UNDP: Mapping the Palm Oil Value Chain Mapping the Palm Oil Value Chain Opportunities for sustainable palm oil in Indonesia and China, 2020.

USDA: Production, Supply and Distribution (PSD) Database - Palm Oil, Washington, DC, 2025.

Vijay, V., Pimm, S. L., Jenkins, C. N., and Smith, S. J.: The impacts of oil palm on recent deforestation and biodiversity loss, PLoS One, 11, https://doi.org/10.1371/journal.pone.0159668, 2016.

de Vos, R. E., Nurfalah, L., Tenorio, F. A., Lim, Y. L., Monzon, J. P., Donough, C. R., Sugianto, H., Dwiyahreni, A. A., Winarni, N. L., Mulani, N., Ramadhan, G., Imran, M. A., Tito, A. P., Sulistiawan, P., Khoirul, M., Farrasati, R., Pradiko, I., Grassini, P., and Slingerland, M.: Shortening harvest interval, reaping benefits? A study on harvest practices in oil palm smallholder farming systems in Indonesia, Agric. Syst., 211, https://doi.org/10.1016/j.agsy.2023.103753, 2023.

Wakhid, N. and Hirano, T.: Soil co2 emissions and net primary production of an oil palm plantation established on tropical peat, Mires and Peat, 27, https://doi.org/10.19189/MaP.2021.OMB.StA.2159, 2021.

Wakhid, N., Hirano, T., Dariah, A., and Agus, F.: Net primary production of oil palm plantations on tropical peat, Mires and Peat, 28, https://doi.org/10.19189/MaP.2021.SNPG.StA.2288, 2022.

Williams, M., Richardson, A. D., Reichstein, M., Stoy, P. C., Peylin, P., Verbeeck, H., Carvalhais, N., Jung, M., Hollinger, D. Y., Kattge, J., Leuning, R., Luo, Y., Tomelleri, E., Trudinger, C. M., and Wang, Y. P.: Improving land surface models with FLUXNET data, Biogeosciences, 6, 1341–1359, https://doi.org/10.5194/bg-6-1341-2009, 2009.

Wiltshire, A. J., Burke, E. J., Chadburn, S. E., Jones, C. D., Cox, P. M., Davies-Barnard, T., Friedlingstein, P., Harper, A. B., Liddicoat, S., Sitch, S., and Zaehle, S.: JULES-CN: a coupled terrestrial carbon–nitrogen scheme (JULES vn5.1), Geosci. Model Dev., 14, 2161–2186, https://doi.org/10.5194/gmd-14-2161-2021, 2021.

Xu, Y., Ciais, P., Yu, L., Li, W., Chen, X., Zhang, H., Yue, C., Kanniah, K., Cracknell, A. P. ;, and Gong, P.: Oil palm modelling in the global land surface model ORCHIDEE-MICT, Geosci. Model Dev., 14, 4573–4592, https://doi.org/10.5194/gmd-14-4573-2021, 2021.

Zhao, J., Wei, X., and Li, L.: The potential for storing carbon by harvested wood products, https://doi.org/10.3389/ffgc.2022.1055410, 16 November 2022.

Zhao, Q., Yu, L., Li, X., Xu, Y., Du, Z., Kanniah, K., Li, C., Cai, W., Lin, H., Peng, D., Zhang, Y., and Gong, P.: The expansion and remaining suitable areas of global oil palm plantations, Global Sustainability, 7, https://doi.org/10.1017/sus.2024.8, 2024.

Zolfagharnassab, S., Shariff, A. R. B. M., Ehsani, R., Jaafar, H. Z., and Aris, I. Bin: Classification of Oil Palm Fresh Fruit Bunches Based on Their Maturity Using Thermal Imaging Technique, Agriculture (Switzerland), 12, https://doi.org/10.3390/agriculture12111779, 2022.